BRNO UNIVERSITY OF TECHNOLOGY

VYSOKÉ UČENÍ TECHNICKÉ V BRNĚ

FACULTY OF MECHANICAL ENGINEERING

FAKULTA STROJNÍHO INŽENÝRSTVÍ

HEAT TRANSFER AND FLUID FLOW LABORATORY

LABORATOŘ PŘENOSU TEPLA A PROUDĚNÍ

LIMIT MODES OF PARTICULATE MATERIALS CLASSIFIERS

LIMITNÍ REŽIMY TŘÍDIČŮ PARTIKULÁRNÍCH LÁTEK

THESES OF DOCTORAL THESIS

TEZE DIZERTAČNÍ PRÁCE

AUTHOR   Ing. Martin Adamčík
AUTOR PRÁCE

SUPERVISOR   doc. Ing. Tomáš Svěrák, CSc.
VEDOUCÍ PRÁCE

BRNO 2017

Keywords

Rotor air classifier, fine particle classification, classifier performance aspects, Tromp curve, operating parameters, particle image velocimetry (PIV), laser diffraction method, numerical simulation (CFD)

Kľúčové slová

Vzduchový triedič s rotorom, triedenie jemných častíc, aspekty výkonu triediča, Trompova krivka, operačné parametre, časticová anemometria na základe štatistického zpracovania obrazu (PIV), metóda laserovej difrakcie, numerická simulácia (CFD)

CONTENTS

1   INTRODUCTION

Air classification is a process where the initial feed material is divided into fractions differing by some physical property like size or density. Size classification is subject of this work and the size is represented by equivalent particle diameter. Air classification realized by dynamic air classifier is one of the most widespread methods. Cut size of the classifier under given operating parameters is a particle with unique size which has 50% chance to be classified into fine or coarse fraction. Its value can be established as balance of forces present in the classifier and acting on a particle with specific diameter. The dominant forces are centrifugal force introduced by rotation of classifier rotor cage and swirling flow pattern, further it is a drag force acting on particle introduced by forced air flow in the classifier and gravitational force acting on particle. Varying operating parameters directly influence flow patterns and eddy formations, their time and size scales which consequentially effect classifier performance. Effects of varying operating parameters on cut size are studied together with effects on the flow field and flow patterns in the classifier.

In the experimental part, flow patterns and velocity vector maps in the near rotor region and in the blade passageway are studied and visualized by particle image velocimetry PIV method. Series of readings are taken and evaluated for combination of different fan and classifier rotor settings. In the second stage of the experimental part, classification trials with barite feed material are carried out. Particle size distributions for fine and coarse fraction are established by laser diffraction method. Performance of the classifier, split ratios and Tromp curves are analysed for different operating parameters. Velocity readings at the inlet to the classifier and particle size distribution of the feed material are measured and used as boundary conditions in the numerical simulations.

Numerical model representing simplified dimensional and geometrical copy of the classifier used in the experiment is created in commercial CFD software Ansys Fluent. Measured physical variables for different operating parameters are used as boundary conditions in several numerical simulations. Results are then compared with data collected in experimental section. Furthermore, particle trajectories are calculated in these simulations and effect of flow field is generalized. Classifiers are often used in the close circuit milling systems so that the particles which comply required cut size can be extracted timely and the over grinding phenomenon is avoided. Ultrafine powder classification techniques play an important role in exploiting the advanced materials. Ultrafine powders possess many special properties and effects which are closely related to their particle size. Rapid development in materials science introduces new and demanding product requirements. To meet the needs of industries such as chemical industry, ceramics or bioengineering, which work with ultrafine powders, it is very important to research on ultrafine pulverising and classification theories and their applications. Classification of particulate materials with sizes below 10 microns is commonly considered as a borderline for effective application of air classifiers across various industries. For the given mass flow rate, the number of particles increases exponentially with decreasing particle size. High tangential velocity of rotor blades, also called tip velocity is required for ultrafine particle classification. It however also has a negative effect of increasing particle residence time and therefore increasing chances of particle agglomeration. Aim of this work is study of air classification method for applications with particle sizes below 10 microns with special focus on turbulent flow field structures and their effects on particle trajectories and final termination points.

2   AIR CLASSIFIERS

The various types of size classifiers fall into two general categories: those that separate by forces of fluid dynamics and those involving the possibility of passing through an aperture. The former is density dependent, whereas particle density considerations do not enter the latter scenario. Fluid dynamic size separation takes advantage of the differences in rates of travel of particles in a fluid arising from differences in particle size. If the rates of travel are also influenced by differences in densities, the separation is terminal sorting. Air classifiers belong to this category [1]. Numerous air classifier designs are described in the literature [1, 2, 3]. This paper will use the systematization of air classifiers which uses the separation zones as presented by Shapiro el al. [1]. Four basic separation zones are known (gravitational-cross flow, gravitational-counter flow, centrifugal-cross flow and centrifugal-counter flow).

3   ROTOR AIR CLASSIFIER

Guo et al. [4] described the dynamic state air classifiers development through three generations, with centrifugal and cyclone classifiers as the first and second-generation classifiers, respectively. The third generation is rotor air classifier. Compared to its predecessors, the advantage of the rotor air classifier is the employment of the rotor cage as the classifier component which can exert a radial forced centrifugal field. As the third generation, this classifier has a high classification precision and good classification performance [4, 5]. Numerous rotor air classifier designs are described in the literature. In the case of this dissertation a rotor air classifier with vertically installed rotor cage, radial blades and no guide vanes installed is used. In such classifier particles enter from the top or particle laden air enters from below and rises upwards into a conical vessel, containing a drive-activated rotor with a cone and rotating blades. These blades whirl the air to create a centrifugal – counter flow separation zone in the upper part of the vessel. These devices are used for separation of fine quartz powder, cement, ground limestone, etc. The space around the blades is arranged to form a centrifugal – cross flow zone. In this zone particle separation occurs. Due to a minimum of momentum exchange between air and solid phases, the centrifugal counter flow air classifier has a high sharpness of cut [6, 7].

4   ROTOR AIR CLASSIFIER PERFORMANCE

4.1 PERFORMANCE MEASURES

Performance of a rotor air classifier can be measured in terms of three major parameters [8]:

        1. The size selectivity increment (ΔS)
        2. The sharpness of the separation (β)
        3. The cut size (d_{50})

4.1.1   Size selectivity increment and sharpness of the separation

In the ideal classification, it would be possible to divide the mixture of sizes into two fractions, such that one lay wholly below a predetermined cut size called fine and that the other lay wholly above it called coarse, Figure 1. Particles with the size equal to the predetermined cut size would have 50% probability of being collected together with either fine or coarse powders [3, 9].
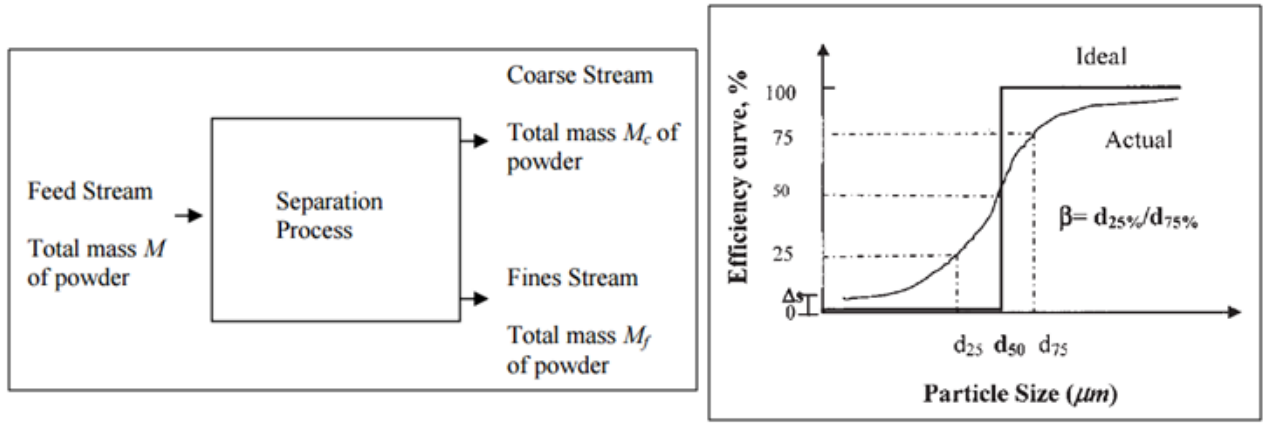
Figure 1 Separation of fine and coarse particles and an ideal and actual efficiency curve in a size classifier [8, 10]

However, such ideal process does not exist due to various stochastic factors such as particle collisions during which the coarse particles can capture fine particles or fine particles can get into the aerodynamic wake formed behind other particles, and thus some fines get into the coarse product and vice versa [1, 8, 11]. The actual classification would generally be represented by typical S-shaped grade efficiency curve, which is related to the size distribution function:

$$G(x) = \frac{M_c f_{cx}}{M f_x}$$ (4.1)

Where G(x) is the grade efficiency and f_{cx} and f_x are the relative frequencies of particles of the size x. The size selectivity S_d is defined as the ratio of the quantity of particles of size d in the coarse fraction to that in the feed. For proper classification, S_d should be low for small particles and high for large particles. Particle size that has 50% probability of getting into the coarse fraction is called cut size – d_{cut} or d_{50}. For an ideal classifier, the $S_d = 0$ for $d < d_{50}$ and $S_d = 1$ for $d > d_{50}$. The size selective coefficient (ΔS) characterizes the quantity of feed material that goes directly into the coarse fraction without classification and is given by the intercept on the abscissa of the extrapolated grade efficiency curve. The sharpness of separation (β) describes the effectiveness of a given classification. It is defined as d_{25}/d_{75}, which is the ratio of particle size with a grade efficiency of 25% to the particle size at 75% grade efficiency. For a perfect classification, it has a value of unity. The smaller the value of β is, the poorer the sharpness of classification [8].

4.1.2 Cut size

The generic mechanism for air classifier is following – the feed material to be classified is suspended in an air stream and the coarse fraction is separated from the fine fraction by the air stream by aerodynamic drag force (F_d), which usually overcomes another force, such as gravitational (F_g), Coriolis (F_{Cor}), or centrifugal (F_c), or their combination [8]. The dominant forces can be considered as: the centrifugal force and the air drag force. A classifier rotor generates centrifugal forces, when particles are accelerated to the peripheral velocity of the rotor. The air drag forces result from the exposure of the particles to the gas flow which is additionally used for pneumatic transport of materials. The centrifugal force (F_c) is defined by.

$$F_c = \frac{m v^2}{r} = \frac{V_p \rho_p v^2}{r} = \frac{4 \pi r_p^3 \rho_p v^2}{3r}$$ (4.2)

3

Where the V_p is the volume of the particle, ρ_p is the density of the particle, m is the mass of the particle, v is the peripheral velocity of the rotor, r is the rotor radius and r_p is the particle radius. The air drag force (F_d) for the spherical shape can be defined from the formula:

$$F_d = \frac{c_d \rho A v_a^2}{2} = \frac{c_d \rho \pi r_p^2 v_a^2}{2} \tag{4.3}$$

Where c_d is the drag coefficient, ρ is the gas density, A is the cross − sectional area of the particle, v_a is the relative velocity between the fluid and the particle and r_p is the particle radius. Considering a spherical particle which is in the balance when exposed to these forces, the derived particle size will be:

$$D_p = \frac{3 c_d r \rho v_a^2}{4 \rho_p v^2} \tag{4.4}$$

As it can be seen, the particle size is primarily dependent on the air and rotor peripheral velocities, which are square in function. Other factors, like drag coefficient or particle and gas density, have less effect on the separation forces. Only when very heavy or very light materials are involved or particle shape varies would there be a significant factor to consider [12, 13, 14]. If the particle is small, the drag force will predominate and the particle will move with the air stream into the fine fraction. If the centrifugal force is greater than the drag force, the particles will be deflected into the coarse fraction. The particle size for which the centrifugal force equals the drag force is called cut size. In principle, if the two forces are equal, the particles will be held in equilibrium. This equilibrium determines the cut size of an ideal classifier [8]. The centrifugal force tends to push the material towards the classifier outer walls. The drag force tends to pull the particles to the rotating cage blades. So, it is the sum of these forces which determines the trajectory of the particles to the coarse outlet or to the fine outlet. The trajectory of the particles is calculated by the integration of the momentum balance of a particle. The equation of motion of a discrete particle is formulated as:

$$\frac{\pi D_p^3}{6} \rho_p \frac{d\vec{u_p}}{dt} = \frac{\pi}{8} C_d \rho D_p^2 |\vec{v_{rel}}| \vec{v_{rel}} + \frac{\pi}{6} D_p^3 \rho_p \vec{g} + m_p \left(-2\vec{\Omega} \times \vec{u_p} \right) +$$

$$+ m_p \left(-\vec{\Omega} \times (\vec{\Omega} \times \vec{r}) \right) \tag{4.5}$$

The first term on the right-hand side represents the drag force ($\vec{F_d}$). C_D is the drag coefficient, ρ_P is the particle density, Dp denotes the particle diameter and the $\vec{v_{rel}}$ is the relative velocity between the fluid and the particle. The second term on the right-hand side represents the gravity force ($\vec{F_g}$) where $\vec{g}$ is the gravity vector. Since the classifier rotor rotates, the Coriolis force and the centrifugal force ($\vec{F_{Cor}}$; $\vec{F_c}$) are taken into account. These are expressed by the two last terms on the right-hand side of the equation, where m_p is the particle mass, $\vec{\Omega}$ is the angular velocity, $\vec{u_p}$ is the particle velocity and $\vec{r}$ denotes the position vector [15, 16].

5 EXPERIMENTAL SETUP

5.1 ROTOR AIR CLASSIFIER

Main parts of the classifier are lower chamber, upper chamber and rotor housing. Internal parts are rotor, bearing and shaft housing and the inner cone. Clean air enters cylindrical lower chamber

via tangential inlet and creates swirling flow pattern. This cyclonic phenomenon is used to separate coarse particles from the air stream. Coarse particles then exit lower chamber through coarse outlet which is connected air tightly to plastic bucket. Inner cone is used to separate lower chamber separation zone from upper chamber separation zone. Air velocity between lower and upper chamber can be adjusted by changing cross sectional area of the inner cone throat. Upper chamber together with inner cone form a cylindrical housing for the centrifugal cross flow separation zone. Feed material enters this separation zone through 2 ports in the top face. It is then mixed with air and different particles are accelerated to their individual terminal velocities through the airflow. Fine particles satisfying classifier cut size parameter are carried into the internal area of rotor whilst coarse particles are rejected and are accelerated towards outer wall. Coarse particles then slide down in the near wall region into lower chamber. Fine particles are carried away from internal area of the rotor through the exit in the rotor housing. Particle image velocimetry method (PIV) is employed to visualize vector field and flow patterns in the selected region of interest. In order to allow equipment to capture flow in the near rotor blades region, modifications to the classifier are carried out. These involve creation of opening in the top face of the classifier to allow the sCMOS camera to gain field of view at the selected region of interest. Camera window opening is then sealed with treated glass to create air tight seal. Inspection opening on the side of the cylindrical body of the classifier is extended to allow double laser head to illuminate the plane intersecting field of interest. Inspection door is modified to provide air tight seal for extended opening in the classifier and a flat surface is created for laser sheet window. Again, this window is sealed with treated glass to provide air tight seal whilst allowing laser illumination. Support frame for laser head and camera was designed as independent structure to isolate machine vibrations from optical equipment. Laser frame then allows two angular and three linear adjustments.

5.2   FAN PERFORMANCE CURVE AND AFFINITY LAWS

Centrifugal fan is a mechanical device with rotating impeller which increases velocity of an air stream. Where the air enters fan axially, then it passes through impeller where the kinetic energy of the impeller is used to displace air radially towards volute casing of the fan. Relationship between static pressure, total pressure and volumetric flow rate of the fan is expressed by the fan performance curve. Some of the important parameters used for fan selection are maximum developed pressure at required volumetric flow rate and particle loading for a certain system resistance curve. Fan affinity laws are a version of the more general similarity laws that apply to all classes of turbomachinery. They express the relationships among the performance variables and can be used to predict performance of the fan, provided that performance at corresponding points of rating for a homologous fan are known. The fan laws can be expressed either based on compressible or incompressible flow conditions and for the given parameters the incompressible version is sufficiently accurate [17].

$$Q_A = Q_B \left(\frac{n_A}{n_B}\right) \tag{5.1}$$

$$P_{AS} = P_{BS} \left(\frac{n_A}{n_B}\right)^2 \tag{5.2}$$

Calculated flow rates are used to establish inlet velocity and these are then compared with measured data to determine boundary condition for CFD simulation. Figure 2 shows relation between different motor supply frequencies, volumetric flow rates and pressure distributions.
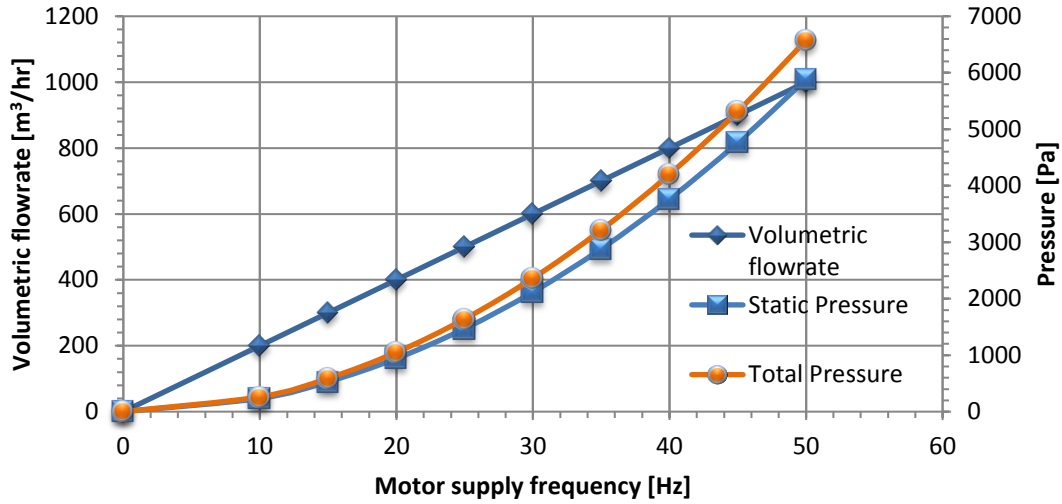
Figure 2 Flow rates, static and total pressure for different fan speeds

Resistance curve of the classifier depends on air velocity magnitude and the resulting higher pressure drop or rotational speed of the classifier rotor. Higher rotational speed translates into greater resistance of the system. Velocity of flow for fluid with known density can be calculated as

$$v_m = \sqrt{\frac{2(P_T - P_S)}{\rho}} \tag{5.3}$$

Where ρ represents density of fluid, P_T represents total pressure, P_S represents static pressure and v_m represents velocity of fluid in the duct. Velocity readings are taken at different positions inside of the duct due to varying velocity distribution in the duct. Velocity in the near wall region is lower than in the core region and therefore resulting measured velocity is calculated as an average of these readings. Figure 3 shows measured air velocities in the inlet duct for 30 and 40 Hz fan speed. It can be observed that velocity increases with decreasing classifier rotor speed. Air velocities calculated for 50 Hz classifier and 30 and 40 Hz fan speed settings are lower than measured values. It can be explained by lower system resistance at 50 Hz classifier speed setting than anticipated by fan performance curve. Velocities were measured without any particle loading which would further increase system resistance and therefore decrease measured velocity.
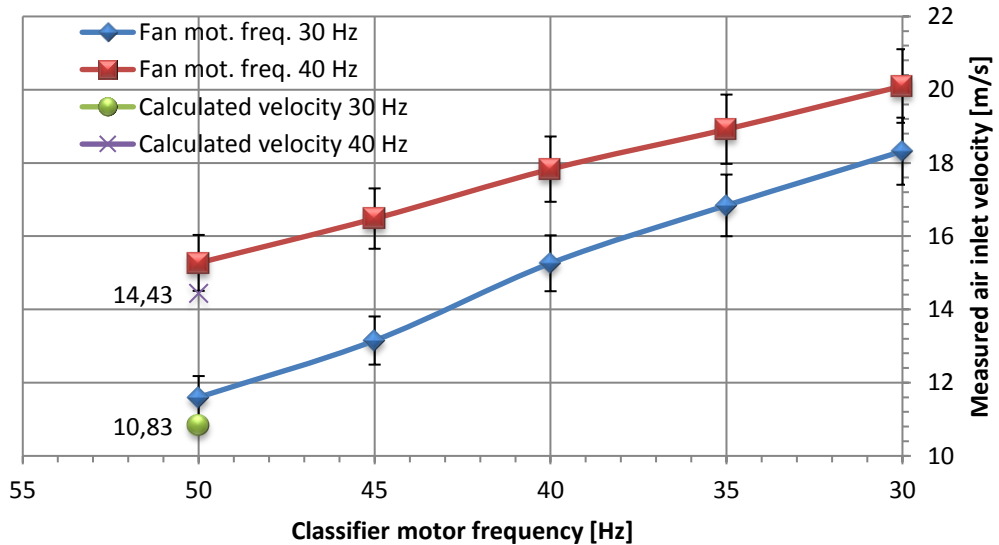

Figure 3 Measured and averaged air velocity in inlet duct

6

5.3   SIZE ANALYSIS OF FEED MATERIAL

Microtrac S3500 employs laser diffraction method with three red lasers arrangement for particle size analysis with improved accuracy. Phenomena of scattered light from light sources projected through a dry state sample delivered as a stream of particles is used. Light rays which strike particles are scattered into form of angular pattern. Angular variation in intensity of light scattered when laser beam passes through a dispersed particulate stream is measured by photo detector array and evaluated.

5.4   PARTICLE IMAGE VELOCIMETRY (PIV)

PIV is an advanced imaging technique allowing capturing and visualizing of instantaneous velocity profiles in the flow in form of vectors, contours, etc. Real time velocity maps are valuable for verification of numerical model predictions as they can capture flow details like small eddy formations as well large-scale flow patterns. Due to physical construction of the device and spatial limitations in situ, 2D planar PIV is used in the experimental section. Investigated area is a plane aligned with expected flow and intersecting rotor blades of the classifier. Experimental setup of 2D PIV consists of several subsystems. Investigated flow must be saturated to specific concentration by seeding particles of certain size. These particles are created by aerosol generator. Particles travelling in the flow are illuminated twice in the plane of laser sheet which determines the investigation plane. Double pulsed laser is used due to its high energy and short pulse capability. Light beam is transformed into a thin sheet by arrangement of spherical and cylindrical lenses. Time interval between the two pulses can be adjusted and it depends on the velocity of the particles. Double shutter camera is used to record light shattered by particles on two frames. Shutter speed is selected in such a way that the second frame captures displacement of original particles from the first frame. It is linked to laser via synchronizer whose main function is to synchronize and trigger both camera shutter and laser pulses. Timing of each frame in sequence together firing of lasers can be controlled with 1 ns accuracy. After successfully exposing camera sensor in two successive frames, the digitized output recordings are transferred into computer memory. Software evaluation of collected data can be essentially described as mapping of average displacements of group of particles. Both frames are divided into a number of small sub areas called interrogation areas. Each interrogation area on the first frame is then compared with interrogation area at the same location on the second frame. Cross correlation technique is then used, resulting into the most probable displacement vector for particular group of particles. This process is repeated for each interrogation area until the complete vector diagram is achieved. Displacement vectors are then converted into velocity vectors based on known time between the laser shots and known physical size of each pixel on the camera. Double exposure camera is designed to capture two frames with a very short time in between them. This inter-framing time represents shutter speed in between two successive frames and it is an important parameter to consider when selecting camera for particle image velocimetry. After the recording process, both images are transferred into connected computer and camera is then prepared for the next pair of images.

6 EXPERIMENTAL RESULTS

Experimental part can be divided into two main sections where the first section focuses on data collected by particle image velocimetry (PIV). It includes velocity vector maps of flow patterns for different operating parameters. These measurements were carried out with oil droplets to provide trustworthy visualization of flow structures. Second chapter includes particle size distributions for fine and coarse fraction obtained in classification trials.

6.1 EXPERIMENTAL PIV FLOW FIELD MEASUREMENTS

Ten data collection campaigns were performed to measure flow field in the rotor cage region and in the blade passageway. Actual position of the rotor cage is not synchronized with the camera sampling frequency due to extended complexity of the measurement and due to limited resources. Therefore, each measuring campaign involves capturing of one thousand pairs of images. Total number of images taken for the spectrum of operating parameters is 20 000. Before the start of measuring campaign, flow domain is seeded by DEHS particles to sufficient level. Operating parameters for fan motor and classifier motor are selected and both are started.

6.1.1 Trial TO6 - Fan motor 40Hz & Classifier motor 30Hz

Initial post processing of raw images is carried out by Davis software:

1. PIV setup with camera allows online real-time transfer of situation in the region of interest during initiation phase. This is not however possible during data collection. Therefore, particle seeding is checked before the measuring campaign is initiated.

2. Classifier and the fan are started and sample image pair is taken with estimated time in between them. Particle displacement vector is then manually evaluated based on the two images. Desired particle shift for further processing should be in region of 4-8 pixels. Time step is adjusted so that particles fulfil the above-mentioned criteria. Measuring campaign is started and one thousand image pairs is collected for the given operating parameters.

3. Sliding background subtraction filter with filter length 8 pixels is used during image pre- processing. It is used because of intensity fluctuations in the background due to reflections. Laser light reflections could not have been prevented due to metal nature of the machine. As a high pass filter, large intensity fluctuations are filtered out while the small intensity fluctuations of the particle signal pass through.

4. Polygonal geometric mask is created at the fixed location of the laser light sheet during PIV processing. Multi-grid interrogation with final window size of 48x48 pixels is defined with 75% overlap and final vector grid spacing of 12 pixels. Each cross-correlation of single pair of interrogation windows results into single displacement vector. All vectors are then combined to form a final 2D vector field of the image.

5. Median filter with interpolation and smoothing for filling up empty spaces after outlier removal are used during PIV post processing.

6. Velocity vectors are recorded in an inertial reference frame. Constant value of velocity is subtracted to transfer vectors from inertial to non-inertial reference frame of the rotor. In reality, the velocity changes with radius. Blades are however narrow and therefore

approximation of the velocity value is acceptable. It is calculated based on blade radius centre value 114 mm and angular velocity for each set of operating parameters.

7. The full set of one thousand image pairs is processed in the above-mentioned fashion. Some of the images are however distorted due to reflections and background noise, some images then display blades interfering with geometric mask. Therefore, images are manually evaluated and inappropriate ones are deleted.

8. Remaining images are then averaged and exported from Davis software as .jpeg and .dat file. Vector field as exported in .jpeg and .dat format from Davis software. It can be observed that the vector field is distorted by laser light reflections along the top left edge of the geometric mask. This is caused by imperfect camera alignment with laser light sheet and by metal nature of the rotor blades.

9. In the next step, the .dat file is imported into Paraview software for further post processing. To visualize vector field and magnitude values, several layers of filters are applied to the imported TECPLOT files. This file represents point values of velocity in X and Y direction. Reference frame is transformed in such a way that its origin is in the bottom left corner of the geometric mask. The selection where the geometric mask is valid is extracted by extract selection conditional filter. Two calculator filters are used to convert point data to vectors and their magnitudes. Threshold filter is applied and tuned to filter out peak values caused by reflections alongside the left and right edge. Glyph filter is used to display vector field with velocity magnitude scale colour map. Delaunay 2D filter is used to map the geometric mask with mesh to display velocity contours in X & Y direction (assumed tangential and radial direction). Another two calculator filters are used to display contours of velocity magnitude in Y direction (radial) and general velocity magnitude. Plot over the line filter is used multiple times to display velocity profiles in Y direction (radial) at programmed locations. And lastly, glyph filter is used to display vector field with Y component scale colour map.

Maximum velocity, radial velocity profiles and 2D vector field

Classifier rotor cage rotates anti-clockwise and therefore the right edge of the image represents leading blade while the left edge represents trailing blade. Blades and their position with respect to coordinate system and eddy formation are indicated in Figure 4. There is 30 blades equi spaced along the circumference of the rotor and are approximately 30 mm deep with 20 mm gap in between them. The air enters blade passageway from the area outside the blades Figure 4 (Y=0-10mm). Here the flow direction is almost tangential with a very weak radial component of the velocity. This is beneficial for particle classification and it has been proven by various researches and experiments. Maximum velocity can be observed in this region and its value is 8.6 m/s. It can be observed that there is a recirculation eddy formed in the area behind the leading blade. It is an area where the airflow has opposite, outward direction. This phenomenon result into restricted passageway in between the blades. As a result, the airflow accelerates in the unrestricted region. As the air enters blade passageway the tangential component of the velocity becomes weaker and the radial becomes dominant component. Figure 5 shows contours of radial velocity where the location with maximum positive and negative radial velocity can be observed. Radial velocity is positive in the unrestricted region of the passageway whilst maximum negative radial velocity can be observed in the recirculation area. Values of radial velocity are plotted over lines which

intersect the passageway by 5 mm increments. The location where radial velocity changes from positive to negative can be established by intersecting profiles with zero value.
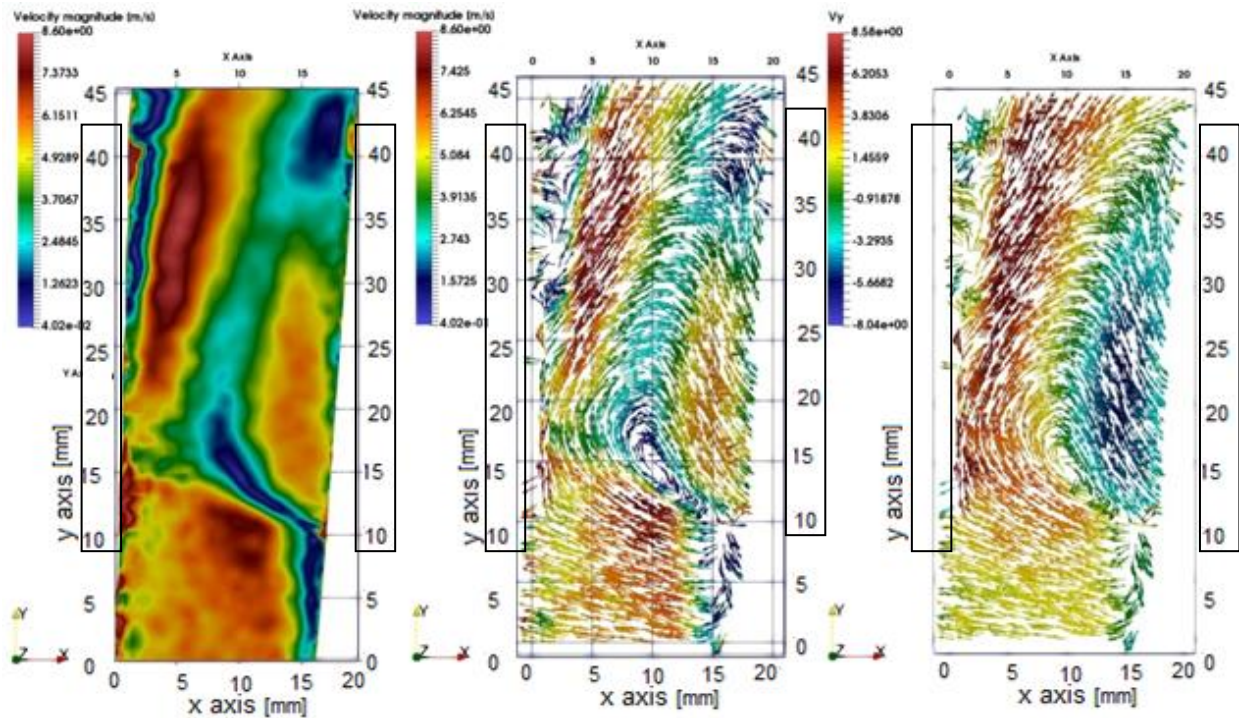

Figure 4 Maximum velocity contour; vector field by max velocity; vector field by radial velocity for 40-30 setting

For the given fan and classifier settings, both positive and negative values reach to +7 and -7 m/s. Velocity profiles are slightly distorted in the proximity of the blades due to laser light reflections and due to imperfect geometric constraints between classifier rotor, laser and the camera. This results into geometric mask which is not completely rectangular.
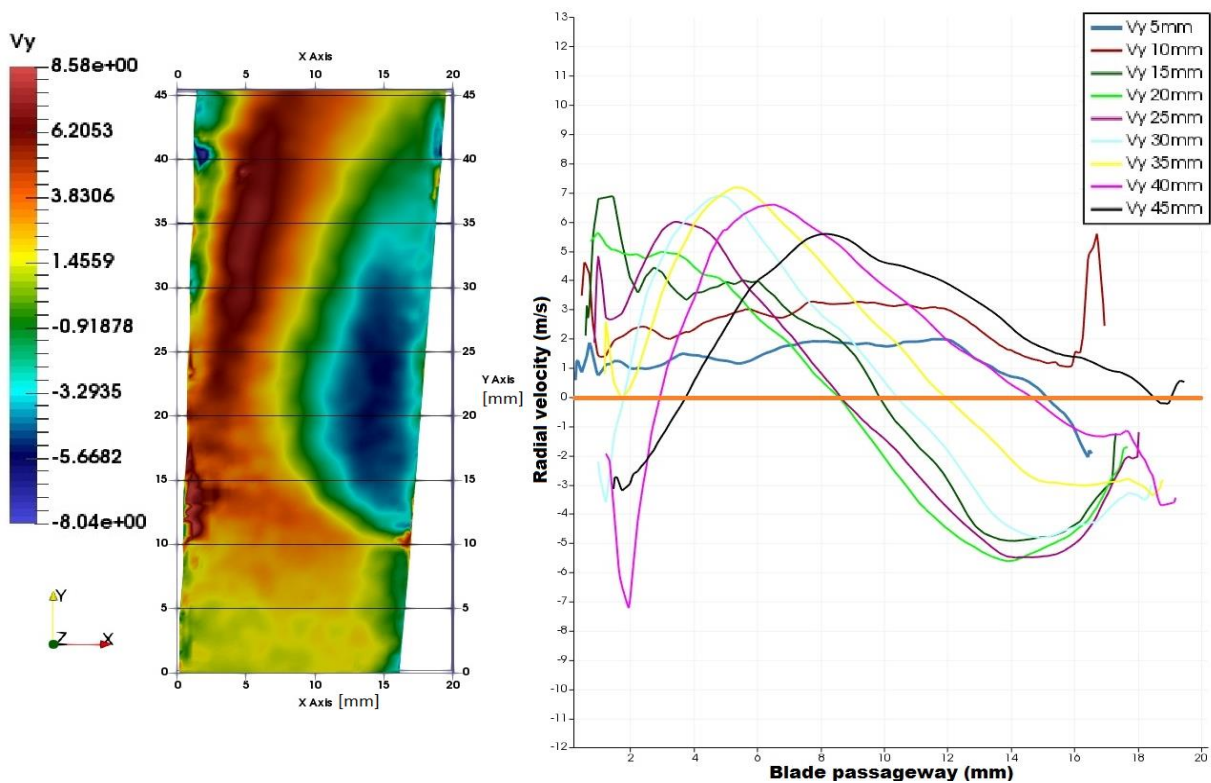

Figure 5 Radial velocity profiles with relation to position in the passageway for 40-30 setting

6.2 PIV RESULTS SUMMARY

All ten measuring campaigns manifest similar flow behaviour with forced vortex forming in the area behind leading rotor blade. This phenomenon results into restricted blade passageway which consequently results into the increased radial velocity in the region before tailing rotor blade. The vortex occupies approximately one half of the passageway and becomes less significant as the air flow enters further in and it diminishes as it approaches exit from the passageway. The maximum velocity is observed for all cases at the inlet to the passageway in the region after leading blade. Tangential component is dominant in this area and as the air proceeds, it becomes less significant and the radial component becomes major component. It has been observed that intensity of this vortex depends on both classifier and fan speed. Higher rotational speed of classifier cage translates into more air being accelerated radially out due to centrifugal force. For constant fan setting, maximum positive and negative radial velocity magnitude increases with increasing classifier speed as shown in Figure 7. Intensity of the vortex and maximum radial velocities also increase with increasing fan speed. Area of the negative radial velocity in the blade passageway is bordered by locations where it changes from positive to negative. These are identified by analysis and filtering of the system and their positions for various operating parameters are plotted with respect to passageway dimensions as shown in Figure 6. For the fan setting at 30 Hz it can be observed that the area of negative radial velocity (eddy recirculation area) decreases in size with increasing classifier rotor cage speed. The most significant size change occurs from 30 Hz to 35 Hz. This trend is less profound for fan setting at 40 Hz. This can be explained by the fact that the PIV camera was not synchronized with classifier rotor position and therefore the recorded data may not completely overlay. Position of the grid has been however adjusted for every investigated case to minimize overlay errors. It is assumed that portion of the particles entering the blade passageway are drawn into the vortex instead of continuing the trajectory into the internal area of rotor and out to fines outlet. This increases chances of particles within the cut size specification to be classified as coarse and therefore decreasing classification efficiency.
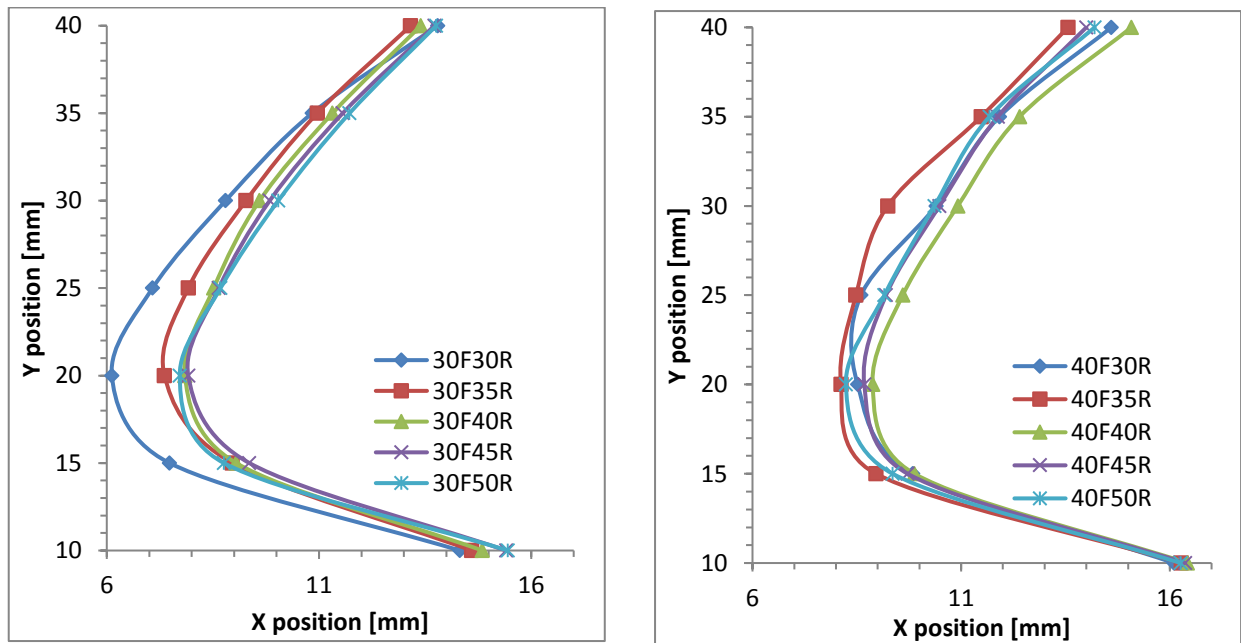

Figure 6 Positions of radial velocity inversion points for different operating parameters

11

Also, some of the oversize particles are classified as fine due to the vortex and therefore decreasing grade efficiency curve. Presence of the vortex in the blade passageway increases resistance of the system to air flow and therefore increasing pressure drop across the classifier. This directly translates into increased energy consumption of the main system fan.
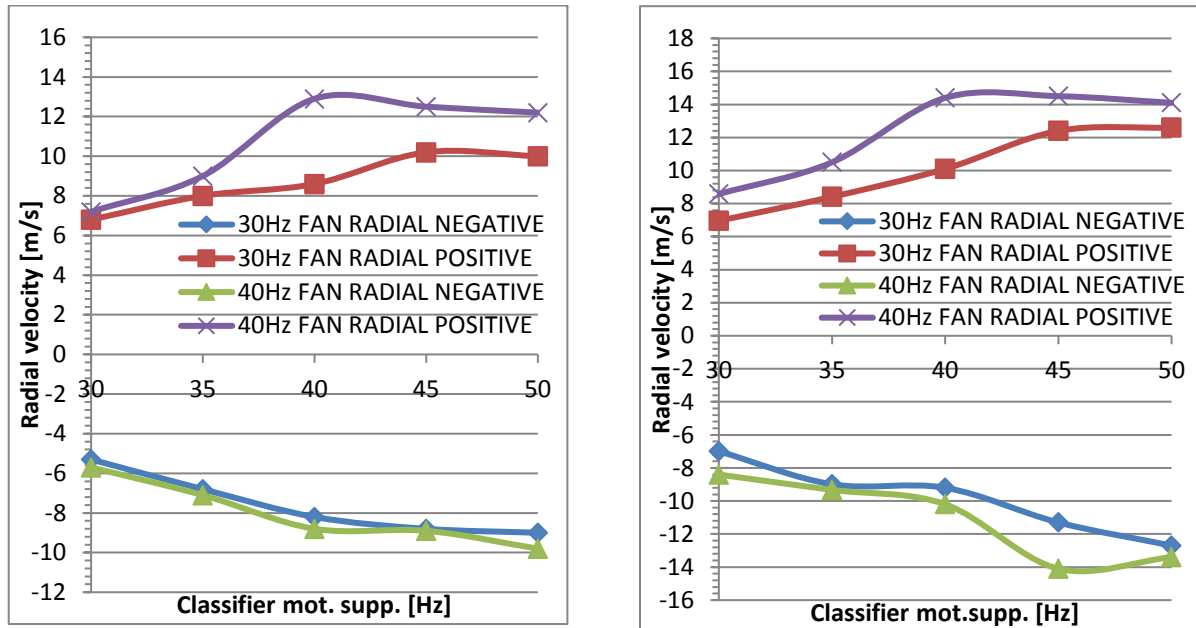

Figure 7 Positive and negative radial velocities on sampled lines and pos. and neg. radial velocities observed

6.3 CLASSIFICATION RESULTS AND LIMIT MODES OF CLASSIFIER

Four groups with three classification trials in each group were carried out to establish effects of varying operating parameters on particle classification in the sub 10-micron range. Main operating parameters affecting classification process and particle size distribution of fine and coarse fraction are identified as classifier rotor cage speed, fan speed and feed rate. Particle size distribution curves for fine and coarse fraction are established by taking 3 measurements for each set of operating parameters and by averaging them. With respect to results of trial TB1, TB2 and TB3 it can be observed that both the number of fines recovered from cyclone and % passing values of fine fraction are decreasing with increasing feed rate as shown in Figure 8. This can be attributed to increased particle loading in the air stream and resulting increased particle-particle interactions. As a result, particles start to agglomerate and form groups of particles. This effectively reduces dispersion and increases weight of the particle group and therefore reduces chances of particles being classified as fines. Increased particle loading increases system resistance and therefore reduces amount of air supplied to the system which consequently reduces number of fine particles recovered from cyclone and also reduces size of major particle distribution points (25%, 50%, 75%, 95%) of the fine fraction. Figure 9 shows influence of different operating parameters of fan and classifier on the number of fines recovered from cyclone and their corresponding 50% passing values. For matching classifier motor settings, influence of increasing fan speed on number of fines can be observed. For all tested classifier speeds the number of recovered fines increased with increasing fan speed.
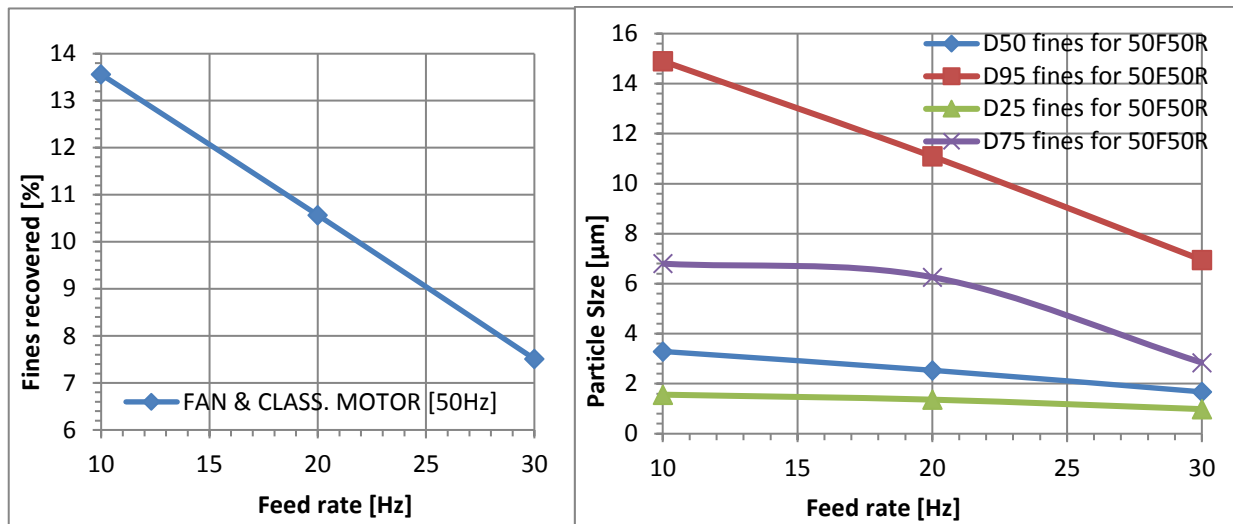
12

Figure 8 Number of fines recovered and fines 50% passing value for varying feed rates (TB1, TB2, TB3)

Greater drag force acting on a particle because of higher fan speed translates into increased cut size of the classifier. The theoretical particle size (cut size) for which two major forces are in balance is now greater in size. Therefore, more particles are able to pass through rotating rotor cage, resulting into greater number of fine particles recovered from the cyclone. It can be observed at the same time that for a constant fan setting and increasing classifier speed, the number of fines is decreasing. Higher tip speed of the rotor cage translates into greater centrifugal force and the resulting theoretical particle size (cut size) for which two major forces are in balance is now smaller in size. Therefore, fewer particles can pass through rotating rotor cage.
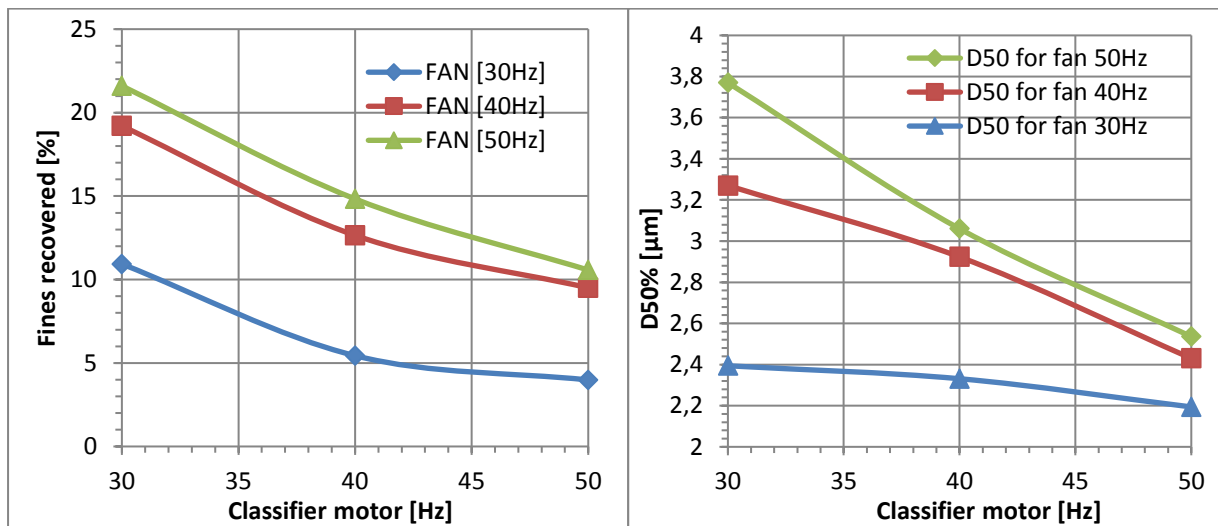

Figure 9 Number of fines recovered and 50% passing particle sizes for varying fan and classifier setting

Achieved 50% passing values for fine fraction are shown in Figure 9. For a constant feed rate of 20 Hz, the finest cut is achieved for operating parameters classifier 50 Hz and fan 30 Hz. The finest cut in all the trials is observed for feed rate setting at 30 Hz and both classifier and fan at 50 Hz. The fines recovery at these settings is however only 9.84%.
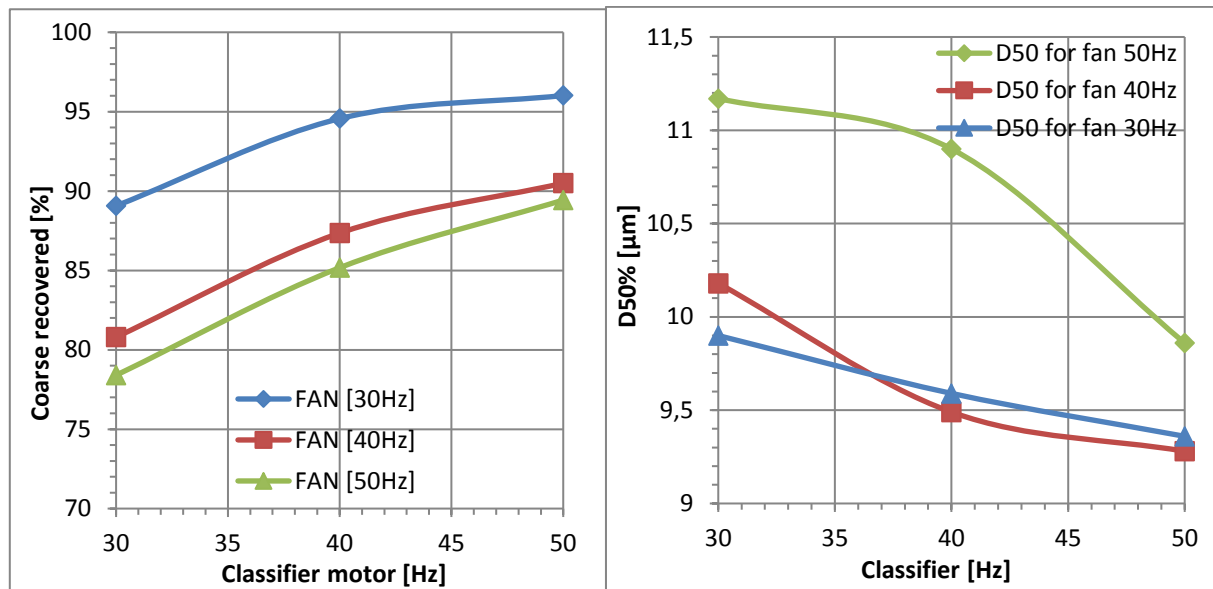
13

Figure 10 Amount of coarse recovered and 50% passing particle sizes for varying fan and classifier setting

The amount of coarse particles recovered in each trial corresponds to conservation of mass law. For identical classifier motor setting, increasing fan speed amounts to a greater drag force acting on a particle and resulting increased cut size of the classifier. Therefore, greater number of particles can pass through rotating rotor cage, resulting into fewer particles classified into coarse fraction. At the same time, for a constant fan setting and increasing classifier speed, the amount of recovered coarse particles increase. Tromp curves or grade efficiency curves are used as one of the tools to evaluate performance of the air classifier. It can be observed on the Tromp curves for different operating parameters that the classification process is not 100% efficient. Tromp values on the y-axis never reach down to 0% and this portion below the curve is called bypass of the classifier. Tromp values can be defined as the ratio of the quantity of particles of size *d* in the coarse fraction to that in the feed. Bypass of the classifier can be defined as a portion of fine material not undergoing classification process and ending in coarse fraction. The bypass fraction is influenced mainly by operating parameters and by classifier design. Increased particle concentration of the air stream increases particle agglomeration and bypass of the classifier. Relation between classifier bypass and feed rate is shown in Figure 11. Here it can be seen that bypass increases with increasing feed rate. Structural parameters of the classifier affect dispersion of the feed material and poor dispersion results into higher bypass. For a constant classifier speed setting, greater airflow through the classifier leads into better dispersion of particles, more efficient classification and thus lower bypass. Cut size of the classifier is however increasing. For a constant fan setting and increasing classifier speed, cut size of the classifier is decreasing at a cost of greater bypass as it can be seen in Figure 11. Set of parameters required to classify particles under 10 microns negatively affects efficiency of classification process. For comparison, typical values of bypass for classification of fines in region of 90% passing 75 microns are typically 10%. Bypass values for trials carried out with varying feed rate were in region of 73%. Bypass values for varying fan and classifier setting varied from 53% to 88%. In order to establish 25%, 50% and 75% passing values the Tromp curve is reduced.
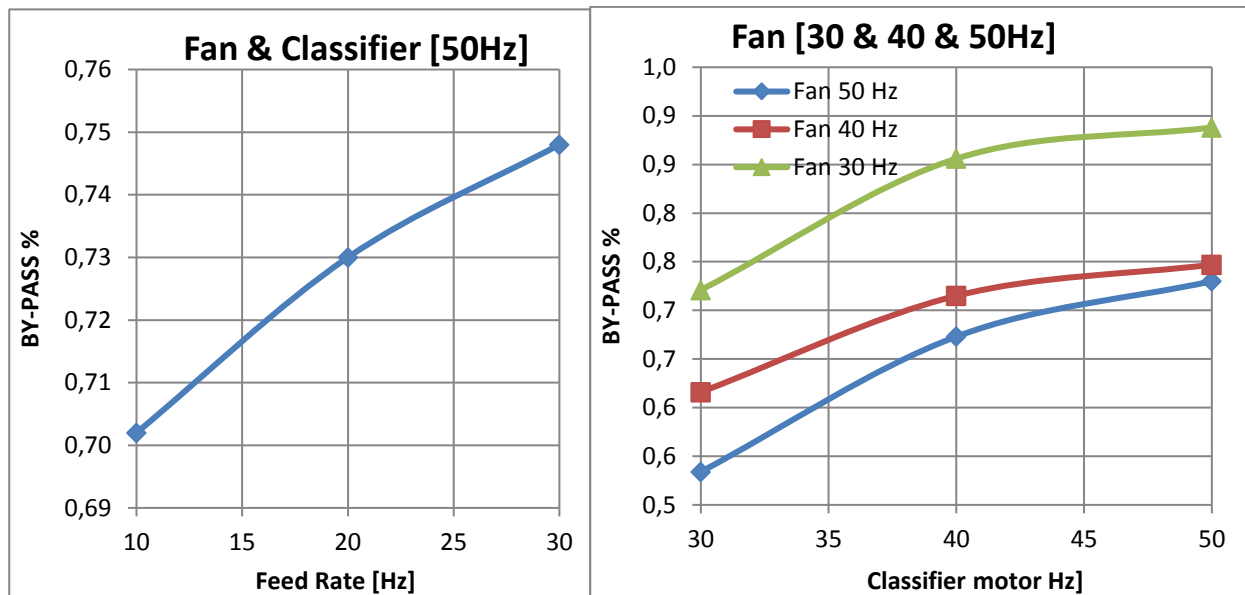
14

Figure 11 By-pass of the classifier for various operating parameters settings

Sharpness of the classification process is represented by β values which are ratio of 25% and 75% passing values with respect to Tromp curves. For an ideal theoretical classification, it has value of unity. The calculated values fluctuate between 0.31 and 0.52. The 50% passing value based on Tromp curve represent particle with specific size for which the forces acting on the particle are in equilibrium and thus the particle has 50% probability of being classified either into fine or coarse fraction. This value represents cut size of the classifier.
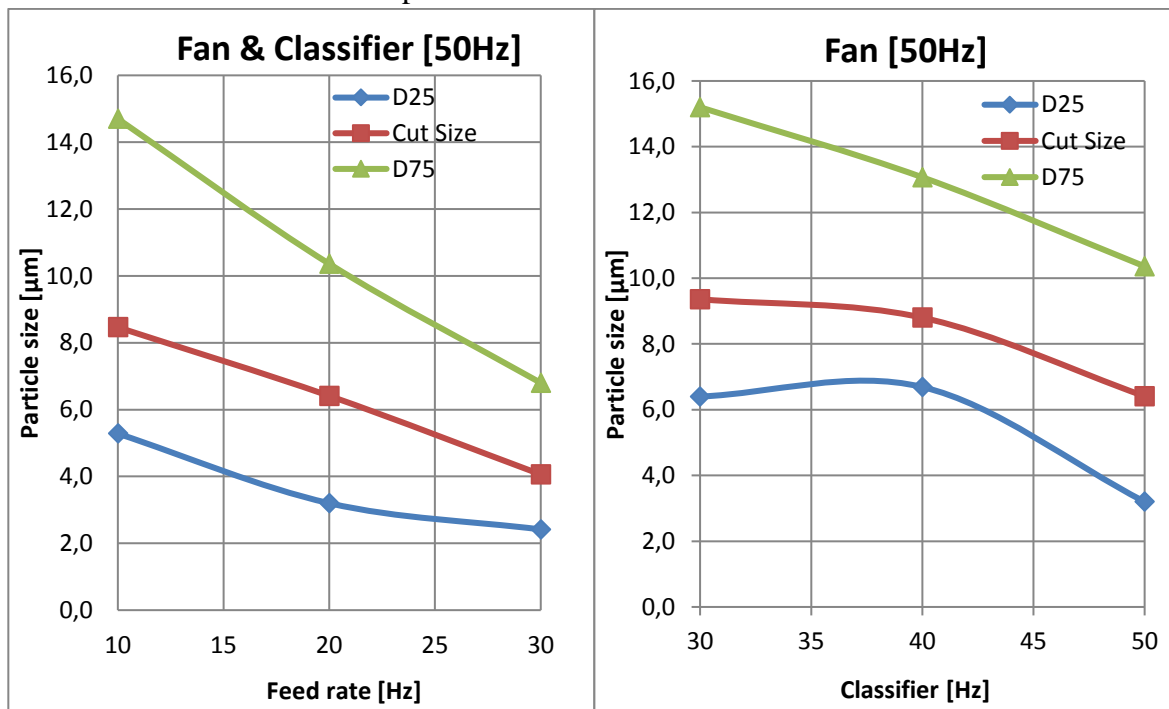

Figure 12 Major % passing values based on Tromp curve for increasing feed rate at constant fan and classifier setting and increasing classifier speed at constant fan and feed rate setting
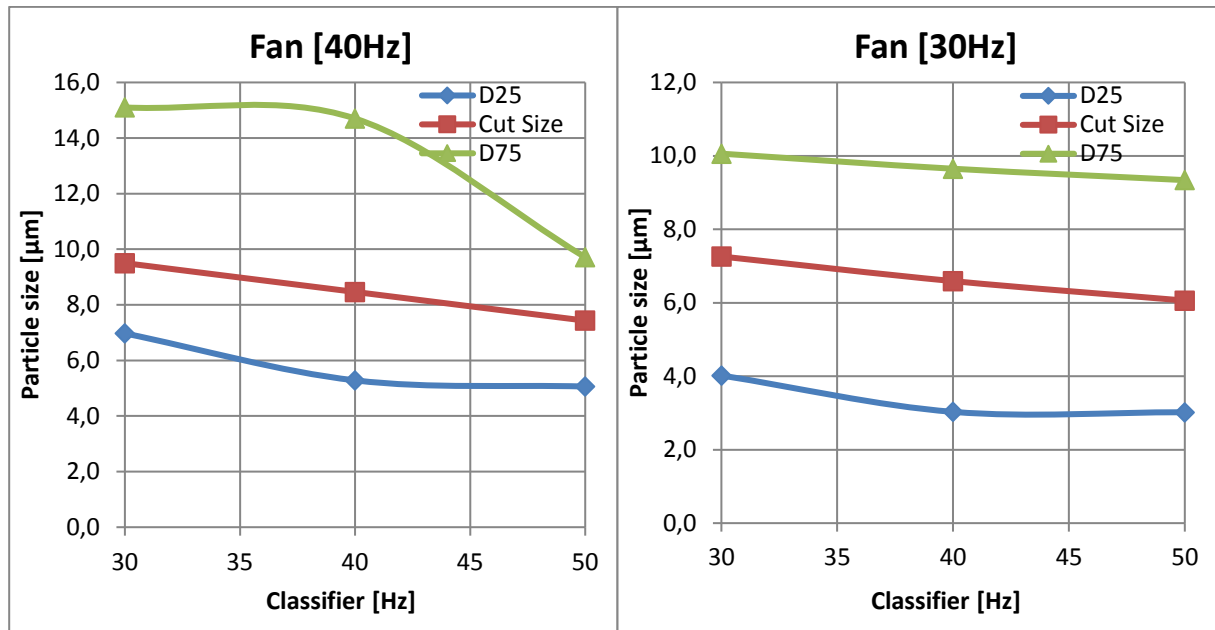
15

Figure 13 Major % passing values from Tromp curve for increasing classifier speed at constant fan and feed rate

It can be concluded that increasing feed rate decreases cut size of the classifier while the difference in sharpness of separation remains insignificant. It can be observed that a rather large increase in classifier speed (from 30 Hz to 50 Hz) corresponds to only a small decrease in cut size, in region of 2 microns.

7   NUMERICAL SIMULATION RESULTS

Individual numerical simulations are carried out for total number of ten cases with varying operating parameters, namely fan and classifier rotor setting. Converged solutions of fluid phase are exported and further post-processed in CFD-POST where the main areas of interest are identified as rotor blades passageway, upper classifying chamber, lower classifying chamber and the inner cone throat. Flow structure is visualized by use of vector maps, positive and negative radial and axial velocity contours. Locations containing flow recirculation zones are illustrated together with velocity magnitudes.

7.1 RADIAL VELOCITY IN BLADE PASSAGEWAY

Grid of nine sampling lines is created over the blade passageway area in order to take readings of desired variables. Passageway selected for sampling is located at 45-degree inclination angle with air inlet duct centreline as this was the exact field of view of the camera in the experimental section. These lines are spaced at every 5 millimetres of passageway depth in the radial direction. Values of positive and negative radial velocity are then plotted across the grid of these lines where for displayed charts, positive component has inward direction. Contours of radial velocities and 3D streamlines for every set of parameters are presented below together with vector map overlay. 3D streamlines are released from internal body - rotor interface surface and are displayed only for the rotating domain and in a non-inertial frame of reference.
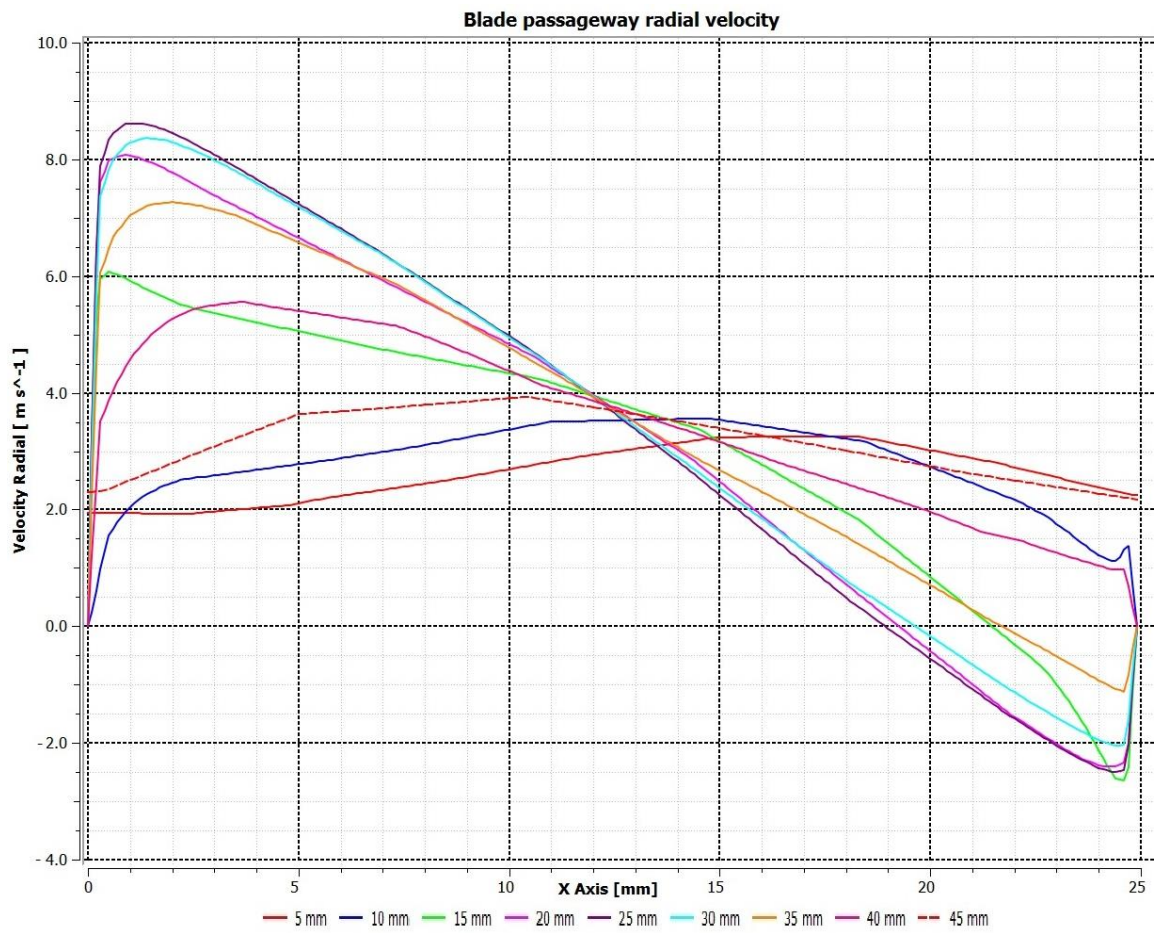
16

Figure 14 Radial velocity profiles for changing position in the blade passageway for 40f-30r setting
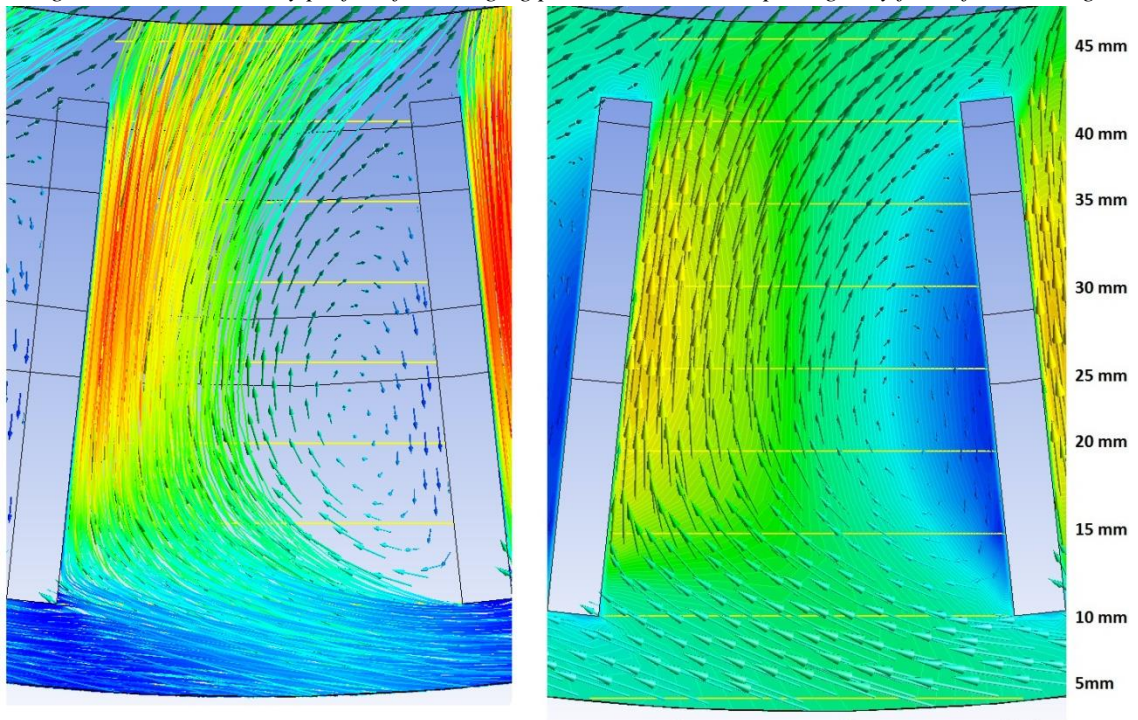

Figure 15 Vector map in examined plane overlaid by streamlines and radial velocity contour for 40f-30r setting

17

7.2 COMPARISON & SUMMARY OF NUMERCIAL RESULTS

Two sets with 30 Hz and 40 Hz fan setting with five simulations in each set for varying rotor speed were carried out. For all the ten cases with anti-clockwise rotor rotation Figure 15 the numerical simulation predicts formation of vortex in the area behind the leading blade. Positive radial velocity is relatively low at the inlet to blade passageway and this can be attributed to swirling nature of the flow in the cylindrical body of the classifier. This flow regime is defined by high tangential velocities and low radial velocities. As the airflow enters the geometrically radial blade passageway, the tangential velocity component diminishes and the radial component becomes major. The radial velocity component of the airflow is further increased due to presence of the recirculation vortex behind the leading blade which restricts flow area in the blade passageway. As the airflow exits the passageway, its radial component becomes minor whilst the tangential component increases. In several cases it was observed that streamlines which exited blade passageway then repeatedly re-entered the following passageway. This is a negative factor as the streamlines represent lines with tangents always parallel to local velocity and therefore mean that some of the air is re-circulating in an undesired pattern.

In all the cases the radial velocity in the area right behind the leading blade is negative with outwards direction. This is a negative factor as the airflow magnitude and direction is one of the two major variables determining fates of the particles. It can be observed that the eye of the vortex is approximately in the centre of the blade passageway.
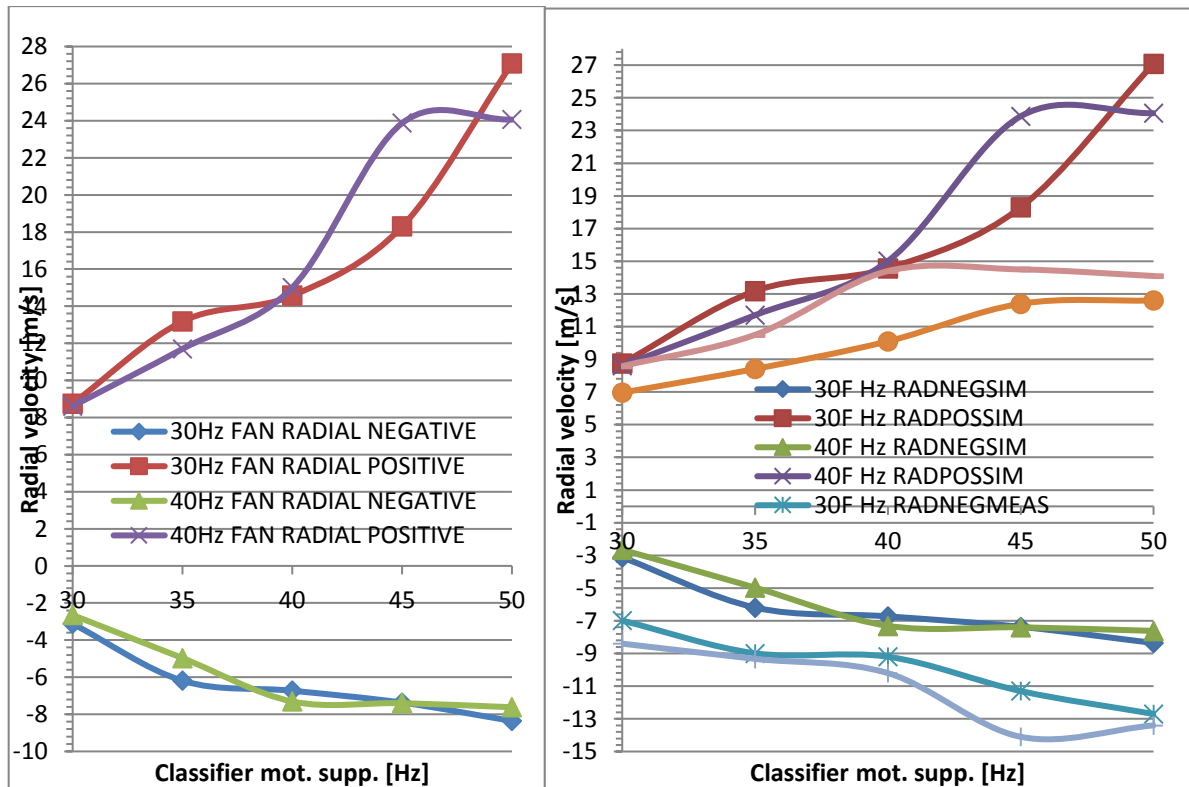

Figure 16 Simulated positive and negative radial velocity and comparison with measured data

Figure 16 shows values of radial velocities obtained from the numerical simulation and their comparison to values obtained by PIV measurement. Numerical simulation correctly predicts

18

increasing magnitude of both positive and negative radial velocity with increasing rotor speed. The actual magnitudes vary due to several possible reasons. It has been found out that radial velocity profiles in different blade passageways vary with geometrical position of the passageway with relation to other geometrical realities and design of the classifier. It has been observed that from total number of 30 passageways, 15 of them were described by more profound vector field with higher velocities whilst the other half of the rotor had radial velocities significantly lower. Intensity of radial velocity changes depending on angular position. This can be noticed not only in the rotor domain but also in the internal body flow domain. This phenomenon has been discovered at all the ten simulations and the author sees several possible explanations for this:

a) Due to high computational cost, the meshing method and size of the control volumes of the mesh for the numerical simulation were optimized in such a way, that the elements are as large as possible whilst maintaining reasonable mesh quality criteria. The elements are not small enough for complex geometrical design of the classifier to form a completely structured mesh. Therefore, some numerical dispersion errors may be introduced into the results, where the numerical solution oscillates around the true solution.

b) Due to high computational cost, all the calculations were carried out as steady simulations and the action of rotor was modelled as a steady state approximation by use of multiple reference frame model. It is possible that the problem is due to turbulence by nature transient and that transient simulation is required to describe changing flow field in the classifier.

c) It was originally assumed that the three-dimensional flow field between classifier inner cone and rotor is pre-dominantly symmetric axially where the considered axis of symmetry was axis of rotation. The 3-dimensional model in this section of the classifier is axially symmetric.
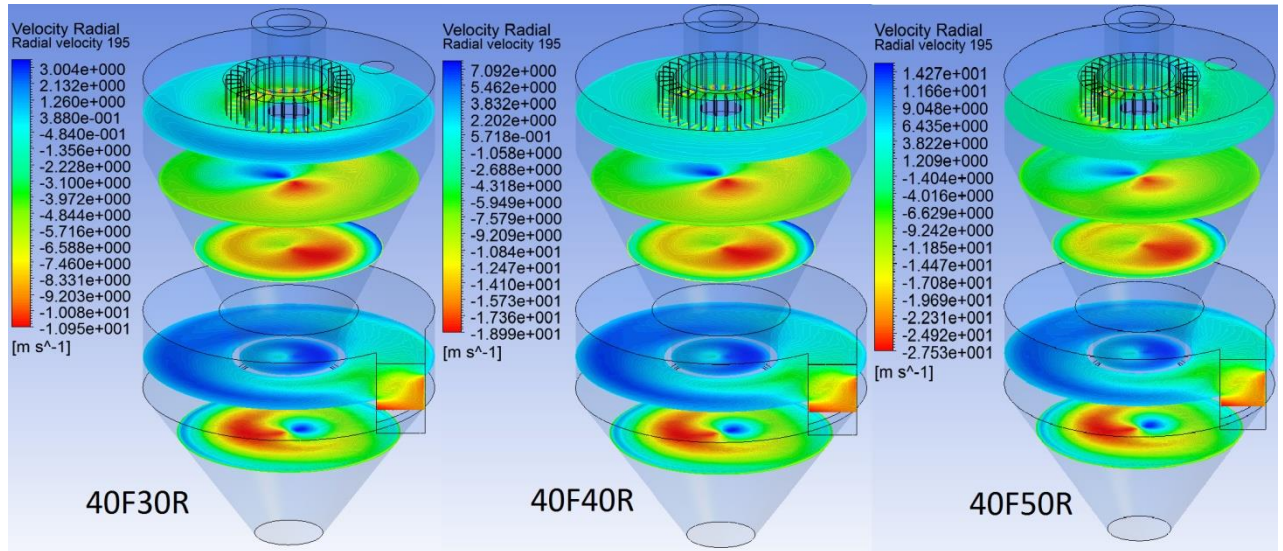

Figure 17 Radial velocity contours for selected settings on horizontal planes at different levels

Contours of radial velocity for selected settings can be seen in Figure 17. For all the below presented figures, positive radial velocity has outward direction. It has been established that the axis of rotation of the swirling flow, even though in cylindrical body, is not concentric with axis of the cylindrical body. Position of the axis of rotation is affected by two factors. First and dominant factor is identified as lip leakage. Bottom section of the classifier has tangential air inlet connected to outlet of the centrifugal fan. The tangential inlet creates swirling flow pattern in the bottom

section of the classifier which is separated from the top section by the inner cone. It was observed that the throat of the inner cone leaks the air into the top section in a specific location. This location further determines position of the axis of the rotation of the swirling flow and consequently determines which half of the classifier top body contains mainly positive and which mainly negative components of radial velocity. Second factor affecting spatial position of the axis of rotation is angular velocity of the rotor. Action of the rotor breaks this pattern apart. This can be noticed mainly in the vertical section of the classifier where the rotor is present. It was observed that increasing rotor speed decreases intensity and the difference between positive and negative component. Furthermore, it centralizes axis of the rotation of the swirling flow.
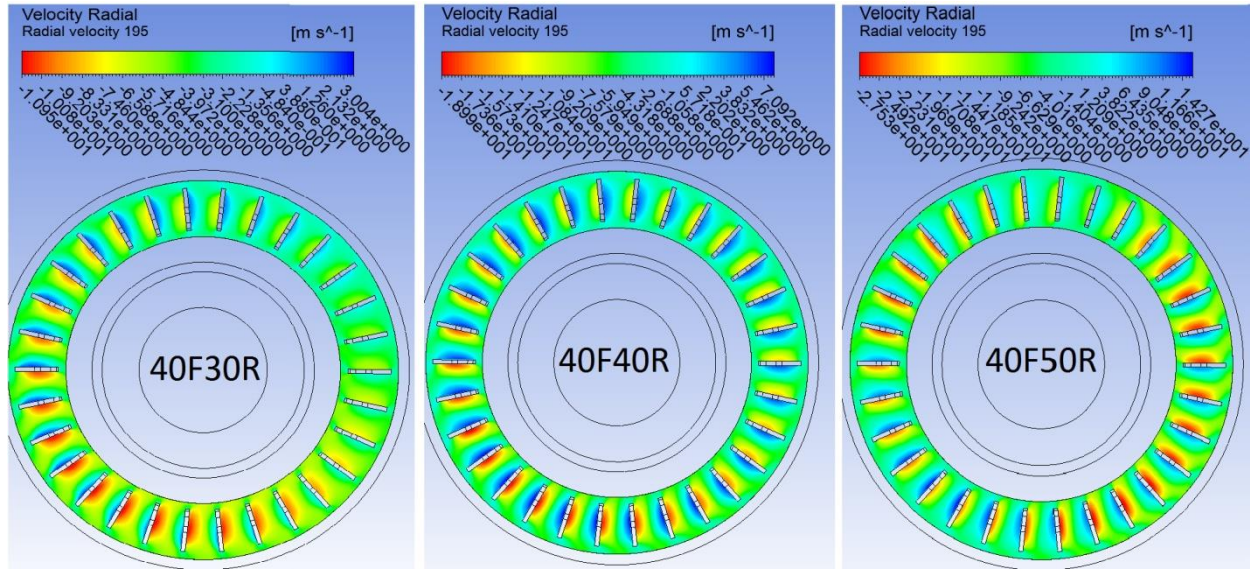
Figure 18 Section through rotor on radial velocity for varying operating parameters

Effects of this pattern are however still present in the rotor domain and are manifesting themselves by uneven distribution of radial velocity in all the blade passageways as shown in Figure 18. Also, it can be observed, that at some locations on the horizontal level of the rotor, the radial velocity is negative and therefore pointed towards walls of the classifier body.

Figure 19 Lip leakage for 40Hz fan speed and 30, 40, 50 Hz rotor speed

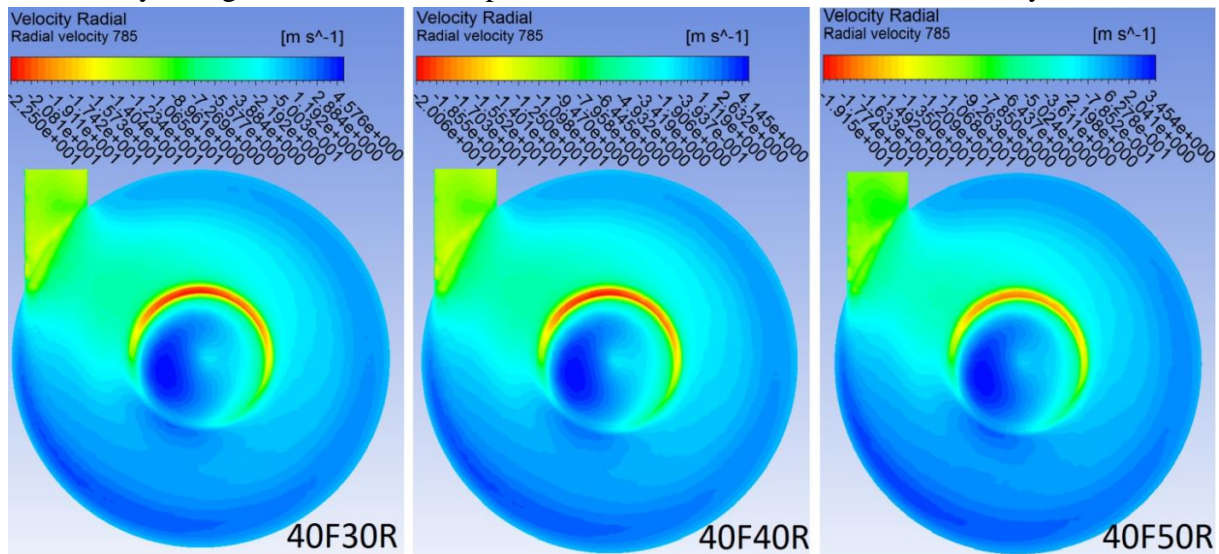Figure 19 shows position of lip leakage in the area 1 mm under the lip of the inner cone throat. It has been noticed that in the lower section of the classifier, the leakage position is determined by position of the tangential air inlet. Radial velocity has decreasing tendency for increasing rotor speed which confirms rotor's effects on axis of the swirling flow described previously.
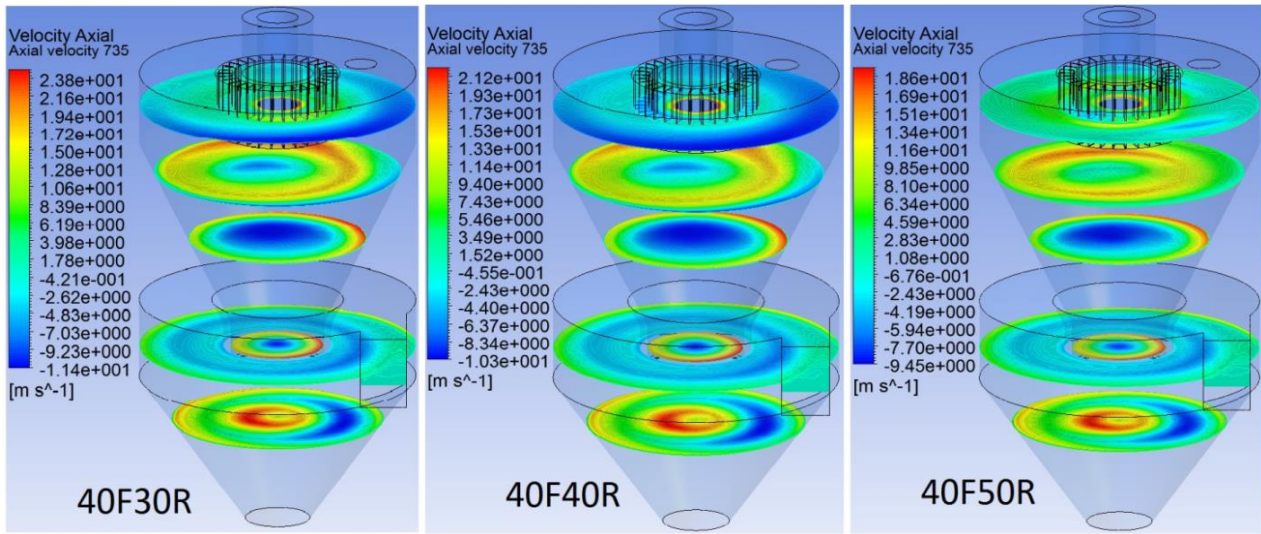

Figure 20 Axial velocity profiles for 40Hz fan and 30, 40, 50Hz rotor

Surface of revolution with 240 mm diameter is created in such a way that it cuts vertically down through rotor blades. Contours of radial velocity are then plotted on this surface for three cases. It can be seen in isometric view of Figure 21 that maximums and minimums of radial velocity vary also depending on vertical position of rotor. The maximum positive values with direction inwards are present in the lower half of the rotor just before trailing blades.
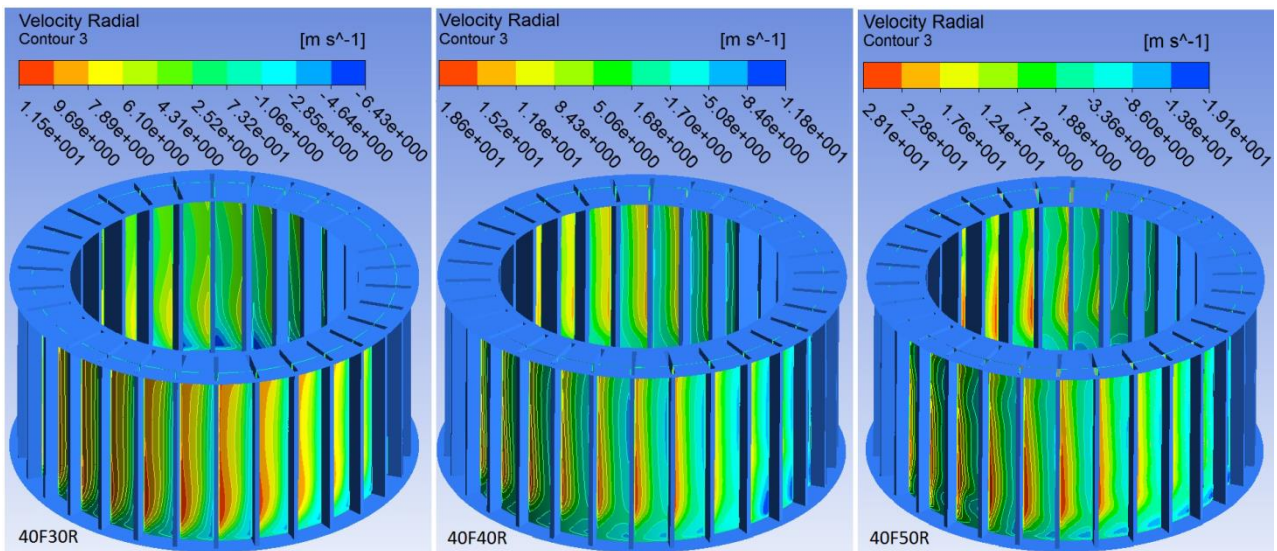

Figure 21 Radial velocity plotted on surface of revolution through rotor blades

Radial velocity profiles and flow patterns in the air classifier were discussed above. Effects of radial and tangential velocity flow patterns on particle trajectories are discussed later in the work. Another component of the flow which has crucial impact on particle trajectories is axial velocity.

Figure 20 shows profiles of axial velocity for different operating parameters. It can be observed that the flow rises axially up in the swirling pattern from the location of the lip leakage and only in the outer layer of the throat in the near wall region. The flow further propagates into conical section of the upper body of the classifier in the swirling pattern in outer layer in the near wall region. There is a point on the outer wall of the classifier where this V-shaped swirling vortex propagating in the upwards direction, separates from the wall and starts heading towards the rotor. Inner surfaces of this vortex do border an area of the classifier where the axial velocity propagates upwards as it can be seen in Figure 22 (green colour for upward axial flow). The axial velocity in the core of this vortex is negative and thus flow occurs downwards, creating a large recirculation zone in the area under the rotor down to lower body of the classifier
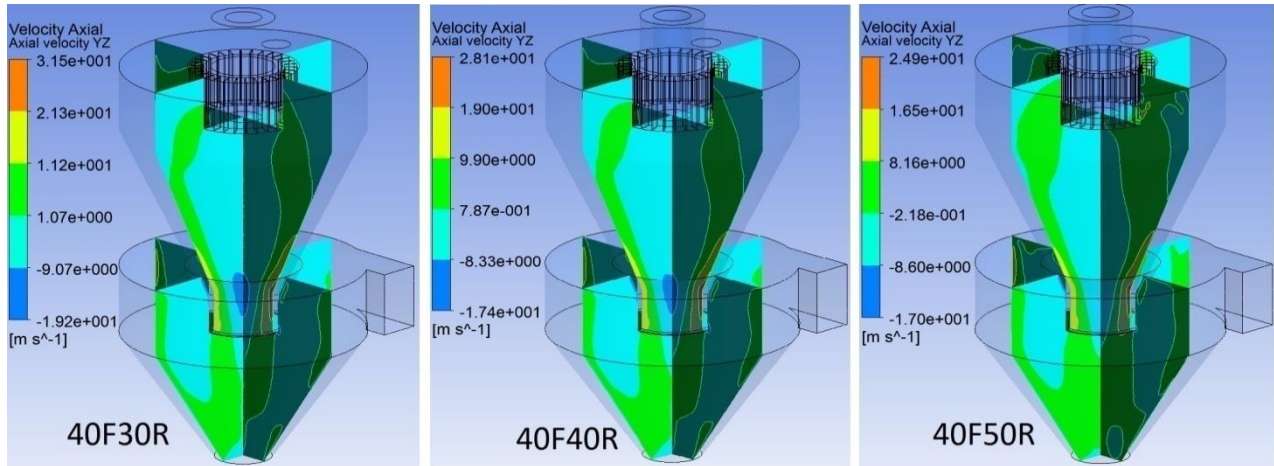

Figure 22 Axial velocities in YZ & XZ plane

7.3   SUMMARY - PARTICLE TRAJECTORIES

Barite particles are tracked and trajectories are visualized to better understand particle behaviour and effects of local flow structures on fate of the particles. Trajectory history is calculated by Ansys Fluent and is then exported into CFD-Post for further post processing. Particles with both spherical and irregular shape were simulated with relation to drag coefficient. No significant difference in particle trajectories was observed and therefore particle trajectories for spherical drag law are presented. Due to high computational cost, particles were tracked in post processing and momentum coupling with continuum phase was not considered. Particles were tracked with limited number of steps to limit computation time due to particles trapped in recirculation zones. Discrete random walk model was used for stochastic tracking to simulate effects of turbulent dispersion. Time constant is selected to be 0,05 and total number of tries for each particle is five. Particles are injected into the classifier through circular surface in the top face of the classifier.

7.3.1   Particle Trajectories for 40F30R Simulation

For the reason of clarity and more distinctive trajectory visualization, particles are divided into two groups by size where the first group only contains particles with sizes below 98% passing diameter. This group represents very fine particles which can pass through the rotating rotor of the classifier. Figure 23 shows particle trajectories for five different particle diameters. Particles are

injected from surface in the top face. Largest particle in the group, 13 microns, is represented by red colour. After entering air flow in the classifier, the particles of this size are dragged by swirling flow and follow spiralling trajectory as they are accelerated towards the outer wall. Some of these particles are repeatedly hit by rotor blades as they try to get inside. It can be observed that a limited number of these particles are able to enter internal area of the rotor. This can be explained by uneven distribution of radial velocity in the area around the rotor, caused by eccentric position of axis of rotation of the swirling flow. It can be also observed that in the other half of the classifier, where radial velocity has negative direction and therefore air does not enter internal area of the rotor, no particles enter this area. On the opposite spectre of particle sizes, the smallest particle in the group, 0.35 microns, is represented by blue colour. These particles readily follow flow patterns and they quickly enter blade passageway area. Here, they progress on a curved trajectory due to curvature of the flow as correctly predicted by simulation and confirmed experimentally by PIV vector map visualizations. No particles below 98% passing size report to coarse fraction due to particle-particle interaction not included in the model.
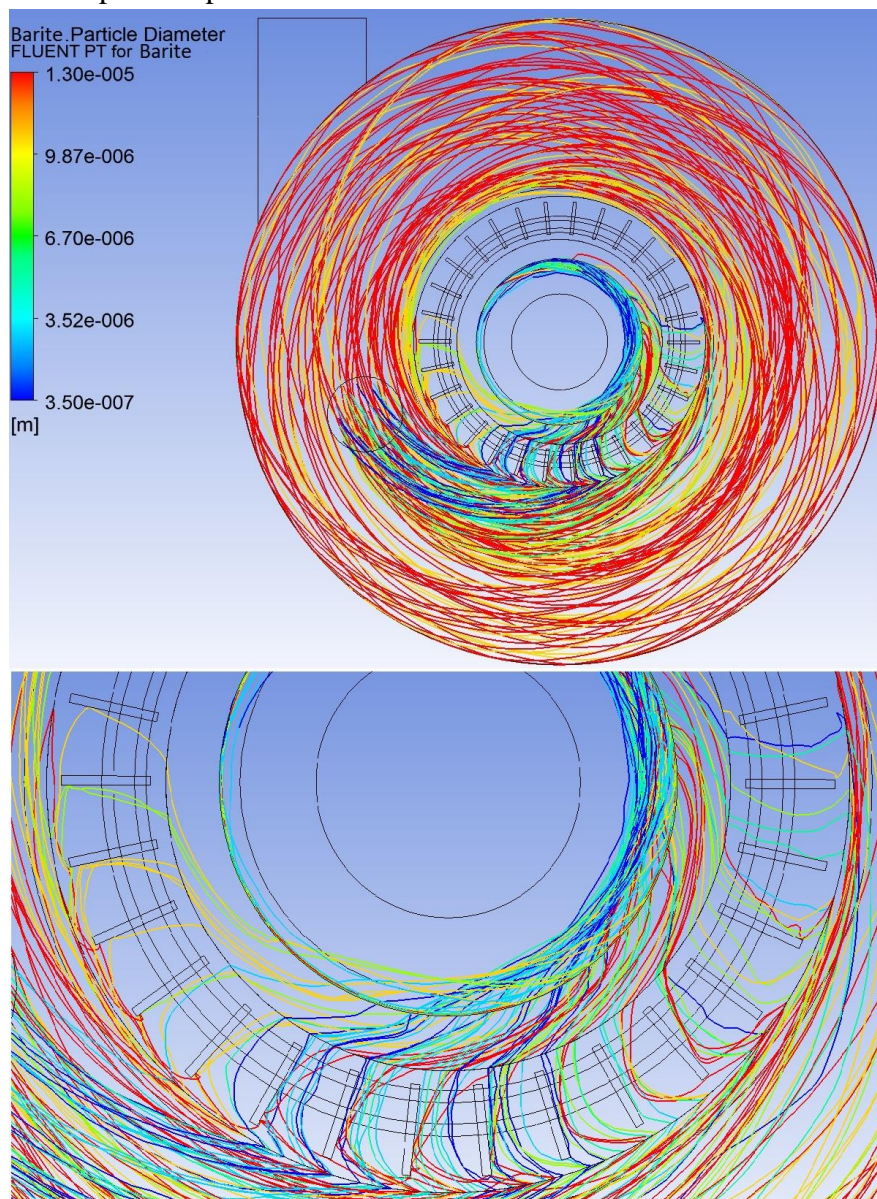

Figure 23 Trajectories of barite particles with 98% passing 13.8 micron for 40F30R

It can be seen in the Figure 24 that almost none of the particles with diameter above 13 microns manage to enter internal area of the rotor. Most of these particles is separated by centrifugal action of the swirling flow and do not even enter proximity of the rotor. There is a significant amount of the particles with sizes up to 42.9 microns re-circulating in the top section of the classifier. These particles would normally follow descending swirling trajectory towards coarse discharge. The largest particles with sizes above 42.9 up to 125 microns start their descending swirling trajectory right after they are injected into the classifier. These particles do not approach proximity of the rotor nor the blade passageway. This is a positive fact as these particles are the most responsible for wear of the blades. Total number of 2195 particles was tracked whilst 166 particles were terminated as escaped and thus classified into fine fraction.
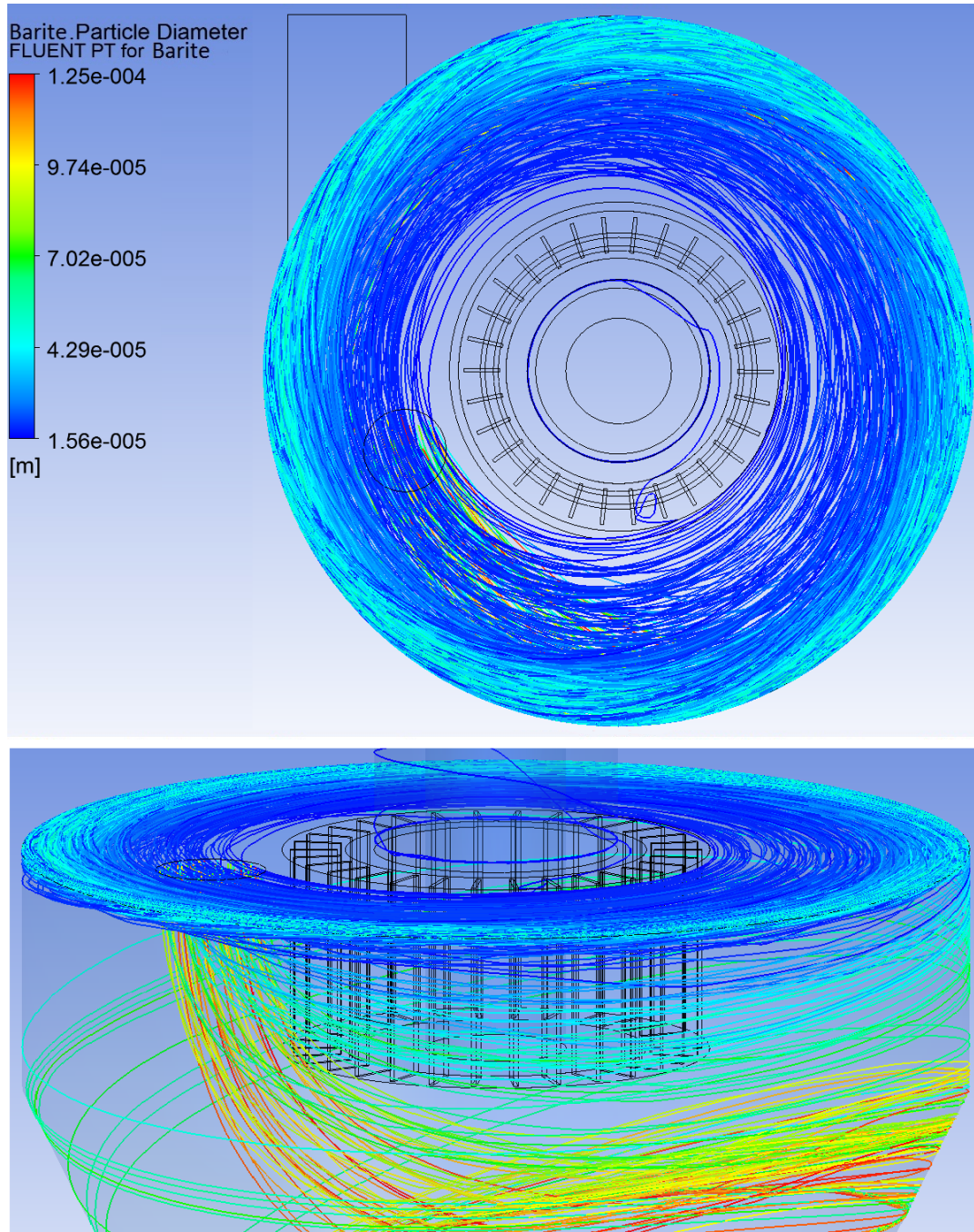

Figure 24 Trajectories of barite particles with size above 13.8 micron for 40F30R

8   SUMMARY

Rotor blade passageway and its proximity is one of the main areas of interest of this work. It is the area where rotor interacts with flow field and with particles and therefore it has crucial significance in particle classification. Particle image velocimetry (PIV) is an advanced method used for visualization of flow patterns and vector maps and for the actual velocity measurements. Modifications carried out to air classifier in order to implement double laser head and high-speed camera for PIV measurements are introduced briefly. Support stands were designed in specific way to allow for laser and camera alignment and calibration where the laser illuminated horizontal plane intersecting classifier rotor whilst camera was installed at the top of the classifier and was focused at the blade passageway. System was then seeded with DEHS oil droplets with submicron particles which were used to reflect light from laser beam. Two consequent images with known delta time between them were taken. These were then split into interrogation windows and based on particle shift within the two windows the displacement vector was calculated and transformed into local velocity vector. In order to describe flow variations in the passageway area for varying operating parameters, 1000 image pairs were taken for 10 sets of parameters as described previously. Therefore, a total number of 20 000 images were taken where each image was in RAW format with approximate size of 30MB making the total size of collected data 600 GB. Images were then post processed and presented in comprehensive sets of contours, vector maps and graphs. A formation of forced vortex is observed in the blade passageway area at all ten cases. Intensity of this vortex increases with increasing rotational speed whilst its size decreases. Distribution of radial velocity in the passageway is such that it reaches positive values (inward direction) alongside the trailing blade whilst it reaches negative values (outward direction) alongside the leading blade, effectively forming a forced vortex. Plane intersecting passageway is overlaid by sampling lines equi spaced after 5mm in radial direction and radial velocities profiles are plotted along these lines. Positive radial velocity becomes a major velocity component in the passageway due to two reasons. Rotor blades are arranged in straight radial pattern and thus directing air in radial fashion and secondly the forced vortex confines passageway area and thus due to conservation of mass law, velocity is increased in the unrestricted area.

It was attempted to carry out PIV velocity measurements also with barite as feed material. Vector maps would have showed velocity vectors of particles in a group rather than flow properties. Injection of compressed air was used to help keep the window for camera and laser clean. It however was not sufficient and the particles completely covered both windows within seconds. Also, due to nature of barite particles, the amount of light reflected was creating an excessive amount of noise to be simply filtered out by camera lens filters and software filtration.

In the second half of experimental section, 11 classification trials were carried out with barite feed material. 300 Kg of barite with particle distribution as required for drilling mud had been provided by client from oil industry and approximately 25 Kg of barite was used in each test. In order to establish split ratio and fines recovery, buckets with fine and coarse fractions were weighed after each test, resulting into 22 weight measurements. Particle size analysis was then carried out to establish distribution curves and major % passing values for both fractions. 3 particle size analyses were carried out for each fraction and these were then averaged to give representative distribution. This amounts into 66 particle distribution analysis and these were carried out by Microtrac which uses laser diffraction principle.

3 tests were carried out with constant fan and classifier setting whilst feed rate was increased for each test. This resulted into decreasing particle sizes which is positive but also into decreased fine particles recovery, Figure 8. It could be explained by increased particle loading in the classifier leading into increased particle interactions. Particles would start creating agglomerates and thus restricting path for smaller particles to be classified as fines and trapping them in these agglomerates. Fines recovery for lowest feed rate was 13.56% whilst for the highest it was 7.51%. Smallest recorded 50% passing size from all the trials was for this setting and its value was 1.674 microns. Operating parameters of the 8 remaining trials were organized in such a way that both influence of rotational speed of classifier rotor and influence of air inlet velocity could have been investigated whilst the feed rate was set to be constant. Three sets of tests were conducted for 30, 40 and 50 Hz centrifugal fan motor settings with 3 trials in each test for 30, 40 and 50 Hz classifier motor setting. Results of all the trials were in good agreement with classification theory and anticipated trends. Major % passing values that are used to describe size distribution of particulate materials were for a constant classifier and feed rate settings and decreasing fan settings also decreasing. Lesser amount of air delivered into the system leads into smaller air velocity and thus smaller drag force acting on a single particle. PIV measurement confirmed that intensity of the forced vortex, thus radial velocities in blade passageway are reducing as seen in Figure 7 effectively leading into finer cut size of the classifier. This trend was recorded for all the cases with the above mentioned operating parameters. It was observed that for very fine particle classification applications, the actual sensitivity of % passing values of fine fraction on fan settings is very low. Change of fan settings from 50 to 40 and from 40 to 30 Hz only resulted in % passing values decrease in range of 0.5 - 1 microns. This is only a very small particle distribution change for a rather significant fan setting alteration. On the other hand, recovery of fine particles decreased significantly, somewhere in region of 10 %, for fan settings decrease from 50 to 30 Hz, as seen in Figure 9.

Major % passing values of particle distribution of fine fraction were decreasing for increasing classifier rotor settings with constant fan and feed rate. Higher classifier rotor tip velocity translates into greater centrifugal force acting on a single particle and also on a volume of fluid. Particles travelling at lower velocity interact with rotor blades which reject and accelerate these particles towards the outer wall of classifier. In the internal body of the classifier, it can be concluded that a higher tip velocity increases tangential velocity and decreases radial velocity of airflow in the classifier body. PIV measurements of flow field in the blade passageway indicate increasing intensity of the forced vortex with increasing rotor speed. This could be explained by increased local mixing of air with both positive and negative radial velocity. Classifier rotor itself can be considered as centrifugal fan and therefore generating airflow against the main fan. Higher rotor speed means greater amount of air flowing in the negative radial direction. Due to conservation of mass flow rate, the intensity of forced vortex is therefore increased. This trend has been observed for all the cases with the above defined operating parameters. It was observed again that for a very fine particle classification, the actual sensitivity of % passing values of fine fraction on rotor settings is very low. Alteration of classifier motor settings from 30 to 40 and from 40 to 50 Hz only resulted in % passing values decrease in a range of 1.5 - 2 microns. This is a minor particle distribution change for a significant rotor speed alteration. Similarly, like the previous cases with decreasing fan setting, increasing rotor speed decreased recovery of fine particles and therefore increased by-pass of the classifier. For alteration of motor supply frequency from 30 to

50 Hz, by-pass increased by approximately 10% as seen in Figure 11. The actual values of by-pass varied between 53% and 88% which means that the classification process is very ineffective. For comparison, by-pass values for a more standard application are usually 10%. Based on the results provided, it can be concluded that for classification of particles with sizes below 10 microns, the actual classification process becomes less and less sensitive to operating parameters like air velocity and rotor tip velocity. The process also becomes very ineffective because of large amounts of fine particles being classified into coarse fraction.

Numerical simulations were carried out using commercially available CFD software Ansys Workbench (Meshing, Fluent and CFD-Post). Each numerical simulation correctly predicts formation of forced vortex in blade passageway. Location of positive radial velocity alongside trailing blade and negative radial velocity alongside leading blade is predicted correctly. Blade passageway was mapped by 9 sampling lines located after 5 mm in radial direction. These lines are in the same position as sampling lines used for mapping during PIV measurements. Radial velocity profiles are ten plotted and compared to measured data. Magnitudes of these velocities are slightly over predicted when compared to PIV measurements, they however exhibit correct trend of increasing vortex intensity for increasing rotor tip velocity. It has been observed that the vortex intensity is not uniform in all the blade passageways. This is explained by inner throat lip leakage position Figure 19 where, as consequence, the axis of rotation of the swirling flow is not coincident with axis of rotation of classifier rotor.

Axial velocity profiles were investigated by cutting classifier by two planes (XZ & YZ) through the centreline as seen in Figure 22. It can be noticed that after the air flow leaks through the lip, it carries on swirling alongside conical surface of the classifier in the upwards direction. There is a point on the conical surface where the flow separates from the wall and carries on towards classifier rotor. This is an area of classifier with positive axial velocity. In the core of the classifier, axial velocity is negative and forms one large recirculation area which overlaps down to bottom section of classifier where the tangential inlet is located. This again has important consequences for particle classification and is discussed later. The axial velocity decreases with increasing rotor speed. It is explained by increased tangential component of the velocity at the expense of reduced radial and axial component.

Barite particles were tracked in the classifier for 3 solved fluid phase solutions. Operating parameters for these selected cases were 40 Hz fan setting and 30, 40 and 50 Hz classifier setting. Particles with size distribution as per classification trials were injected into the classifier through a surface in the top face of the classifier. In order to add clarity to trajectory visualizations these were filtered by size corresponding to 98% passing diameter. Simulation correctly predicted particle behaviour where particles of different sizes followed different and anticipated trajectories. Smallest particles from the feed were able to enter internal area of the rotor, thus were classified into fine fraction. Particles with larger diameter were not able to enter either due to swirling flow and consequent cyclonic action or due to interaction with rotor blades which rejected those oversized particles. In general, there was a good agreement between predicted maximum particle size able to pass through the rotor and actual measured maximum particle size that passed through the rotor during classification trials. As a reflection of results of predicted particle trajectories and of measured and simulated flow patterns inside of the air classifier, there appear to be negative factors attached to these flow realities which limit performance of the classifier and its capability to classify even smaller particles. These are summarized below:

- Radial velocity component of the swirling flow in the upper part of the classifier, in the area between rotor blades and outer wall, is not always positive (inward oriented). This means that after the particles are injected, there is a portion of even fine particles that is accelerated towards outer wall of the classifier and not towards the rotor. This fact effectively limits chances of these particles to be classified as fines which increases by-pass and thus decreases classification efficiency.
- As the particles follow swirling descending trajectory around inner wall of the classifier and towards throat of the inner cone, they cross an area where the flow separates from the conical section of classifier body towards rotor blades. Increased particle concentration around the wall leads into greater amount of swirling consistent mass with greater momentum. It has been observed that these particles which contain portion of the fines are unable to separate from the wall in the region of the flow separation. This again increases by-pass and decreases classification efficiency.
- Particles that are able to separate from the near wall region and find their way into core may then get trapped in the recirculation area present under the classifier rotor. As an effect, recirculation areas increase particle concentration in the flow which consequently increases chances for particle-particle interactions and possible agglomeration. Axial velocity in the core of the classifier takes negative values and thus accelerates particles towards bottom of the classifier where the coarse fraction outlet is located. Fine particles that enter lower section of the classifier body with tangential air inlet very rarely find their way back up to be classified as fines. This again increases by-pass and decreases classification efficiency.
- Due to non-uniform radial and tangential velocity distribution in the area around the rotor, particles of the same size may be approaching rotor with different velocities. Some of the particles with size close to cut size may then pass through the rotor blades whilst some may not. This reduces sharpness of separation of the classification process.
- Radial velocities in all the blade passageways are even less uniform due to misaligned axis of rotation of the swirling flow. This leads to positive and negative radial velocities in each half of the passageways. This reduces sharpness of separation of classification.
- Forced vortex is formed in the blade passageway area due to nature of straight, radially oriented blades. This vortex acts like recirculation area and it has been observed that some of the particles were trapped in here, whilst some of the fine particles were sucked and accelerated in the negative radial direction. Intensity of this vortex increases with increasing rotor speed which is essential for ultra-fine particle classification. Some portion of fine particles is rejected into coarse fraction due to this and thus increasing by-pass and decreasing classification efficiency. This vortex also increases tangential velocity at the entry point to the blade passageway and therefore excessively accelerating particles towards rotor blades which increases wear rate.
- For lower classifier rotor speeds, smallest particles were immediately escaping classifier body into fine fraction. Increasing rotational speed of rotor (required for ultrafine classification) essentially increases tangential velocity in the area outside of the rotor and decreases radial velocity in this area. This is a positive phenomenon for ultrafine particle classification. However due to this, even the ultrafine particles follow several revolutions around the rotor before they attempted to pass through the rotor blade

passageway. Therefore, ultra-fine particle residence time in classifier is increased which increases chances of particle agglomeration in the classifier and thus reduces classification efficiency.

Limits of air classification method for classification of particles below 10 microns in size can be lowered by 2 groups of measures. First group represents operating parameters of the classifier and current technical design possibilities:

- Maximum rotor tip velocity used during experiments was 42 m/s which translate to 2975 RPM. This was the limit of technical possibilities of the classifier. Higher tip velocity increases centrifugal force acting on the particle which leads into finer cut size.
- Minimum tangential inlet air velocity used during experiments was 11.6 m/s. Lower air velocity decreases drag force acting on the particle which leads into finer cut size.
- Higher feed rate of particles into the classifier results into increased particle-particle interaction and agglomeration. These agglomerated groups of particles act as barriers for smaller particles which lead into finer cut size of the classifier. The classification efficiency is however significantly compromised.
- It can be seen in equation 4.4 that cut size depends on air density. Therefore, finer cut size can be achieved by reducing density of the air used in the classification process.

Second group represents structural parameters of the classifier:

- Forced vortex which originates in the blade passageway due to rotor rotation can be minimized by optimized blade design. Inclined or curved blade geometry decreases effects of centrifugal action on volume of air.
- Flow field recirculation areas originate in the classifier due to design and fabrication imperfections. These increase particle residence in the classifier. Recirculation zones can be identified by CFD software simulation and structural parameter optimization.
- Tangential air inlet creates non-uniform swirling flow field which results into non-uniform radial velocity distribution in the blade passageways. Multiple tangential air inlets would increase concentricity of swirling flow and classifier body and thus improve radial velocity distributions
- Increased number of discrete phase feed inlets results into better dispersion of particles around the classifier rotor and thus increasing efficiency of classification process.
- Trajectories and residence time of particles under 2 microns were increased in length and time due to high tangential swirling flow velocities and low radial flow velocities. Ultrafine particle classification is sensitive to structural parameters. Closer position of feed inlets to classifier rotor results into shorter residence time and therefore smaller chance of particle agglomeration.

Combination of all the above-mentioned measures must be applied during classifier design process and operation to move limits of air classification method towards submicron particle classification. This work comprehensively analyses the most important factors affecting particle classification process and decomposes these factors onto their root effects. State of the art visualization technique was used to measure, visualize and analyse flow field and actual velocity profiles and magnitudes. CFD simulations were carried out to further investigate flow patterns.

9 LITERATURE

[1]   Shapiro, M., Galperin, V. (2005). *Air classification of solid particles: a review*. In: Chemical Engineering and Processing, vol. 44, pp. 279-285.

[2]   Klumpar, I., V., Currier, F., N., Ring, T., A. (1986). *Air Classifiers*. In: Chemical Engineering, pp 77-92.

[3]   Powtech 83: *Particle technology* – (The Institute of Chemical Engineers symposium series, ISSN 0307 – 0492, 69).

[4]   Guo, L., Liu, J., Liu, S., Wang, J. (2007). *Velocity measurements and flow field characteristic analyses in a rotor air classifier*. In: Powder Technology, vol. 178, pp. 10-16.

[5]   Feng, Y., Liu, J., Liu, S. (2008). *Effects of operating parameters on flow field in a rotor air classifier*. In: Minerals Engineering, vol. 21, pp. 598-604.

[6]   Galk, J., Peukert, W., Krahnen, J. (1999). *Industrial classification in a new impeller wheel classifier*. In: Powder Technology, vol. 105, pp. 186-189.

[7]   Leschonski, K. (1996). *Classification of particles in the submicron range in an impeller wheel air classifier*. In: KONA Powder and Particle Journal, no. 14, pp. 52-60.

[8]   Karunakumari, L., Eswaraiah, C., Jayanti, S., Narayanan, S., S. (2005). *Experimental and numerical study of a rotating wheel air classifier*. In: American Institute of Chemical Engineers Journal, vol. 51, no. 3, pp. 776-790.

[9]   Yu, Y., Liu, J., Zhang, K. (2014). *Establishment of a prediction model for the cut size of rotor air classifier.* In: Powder Technology, vol. 254, pp. 274-280.

[10] Chase, G., G., (2012). Solids notes 11. The University of Akron

[11] Holdich, R., G. (2002). *Fundamentals of Particle Technology*. Midland Information Technology and Publishing.

[12] Hideghéty, A. (2013). *Suspension flow modelling*. Master Thesis, Brno University of Technology, Faculty of Mechanical Engineering, Energy Institute.

[13] Johansen, S., T., Silva, S., R. (1996). *Some considerations regarding optimum flow fields for centrifugal air classification.* In: International Journal of Mineral Processing, vol. 44-45, pp. 703-721.

[14] Kolacz, J. (2002). *Investigating flow conditions in dynamic air classification*. In: Minerals Engineering, vol. 15, pp. 131-138.

[15] Guizani, R., Mokni, I., Mhiri, H., Bournot, P. (2014). *CFD modelling and analysis of the fish-hook effect on the rotor separator's efficiency*. In: Powder Technology, vol. 264, pp. 149-157.

[16] Toneva, P., Wirth, K., Peukert, W. (2011). *Grinding in an air classifier mill – part II: Characterisation of the two-phase flow.* In: Powder Technology, vol. 211, pp. 28-37.

[17] Buffalo Forge Company, Edited by Robert Jorgensen (1983). *An Engineer's Handbook On Fans and Their Applications, Eighth Edition.* In: Fan Engineering, Buffalo New York